APPLICATIONS OF MICRO-ELECTRODES TO ELECTROCHEMICAL KINETICS

A Thesis submitted to the University of

Southampton for the degree of

Master of Philosophy

by

Henry Yuk-shing LUI

NOVEMBER 1975

ABSTRACT

FACULTY OF SCIENCE

CHEMISTRY

Master of Philosophy

APPLICATION OF MICRO-ELECTRODES TO ELECTROCHEMICAL KINETICS

By Henry Yuk-shing LUI

The whole of the work reported in this thesis is concerned with the kinetics of organic electrochemical reactions.

The first part describes the development of a new quasi-steady state method for measuring the kinetics of fast electron transfer reactions using slow linear sweep voltammetry on lead and indium microelectrodes of very small dimensions. Procedures for making electrodes having radii down to 0.1μ are described. The mathematical theory applicable to electrodes of such dimensions is outlined and it is shown that it should be possible to evaluate the standard rate constant for fast electron transfer reactions by using very slow sweep rates. In contrast to relaxation techniques on planar electrodes, the method relies on the fact that the mass transfer in a spherical diffusion field surrounding a microelectrode of radius r is determined in the steady state by the parameter $\frac{D}{r}$ (where D is the diffusion coefficient); for electrodes of r $\sim 10^{-5}$cm it becomes feasible to measure rate constants in excess of 1 cms^{-1} in the steady state. Conventional cyclic voltammetric data

has been used to study a series of polycyclic aromatic hydrocarbons on platinum electrodes and the technique developed has been applied to the perylene/ perylene$^{\cdot -}$ system on indium microelectrodes. It is shown that for this system $k_o \sim 3cms^{-1}$ while the transfer coefficient $\alpha = 0.5$

The second part of the thsies describes work which was carried out in the first year. This was aimed at extending the synthetic applications of the Brown-Walker reaction using pulse electrolysis methods to first generate radicals from a monoester of a dicarboxylic acids, followed by reduction of the adsorbed radicals to carbanionic intermediates.

ACKNOWLEDGEMENTS

I would like to thank my supervisor, Professor Martin Fleischmann for giving me the opportunity to carry out this work, and for his encouragement, inspiration, advice and numerous fruitful discussions; to Dr. David Masheder for his guidance and helpful discussions and especially to Dr. Alan Bewick for his guidance and discussions.

My thanks are also due to all members of the Electrochemistry Group, particularly Dr. C. Smith, T. Young and C. Godden for their help with my practical problems. I would also like to thank Mrs. Welfare for her help in typing part of this thesis.

Finally, I would like to acknowledge the encouragement and support of my parents, brother and sister and my fiancée.

CONTENTS

CHAPTER I

The whole of the work reported in this thesis is concerned with the kinetics of organic electrochemical reactions.

The thesis consists of two parts; the first is a new voltammetric study of the reduction of aromatic hydrocarbons using very small (micro-) electrodes in an attempt to develop a new-quasi-steady state method for measuring the kinetics of fast reactions. This work is described in the first four chapters. Chapter one is a brief literature survey of voltammetry and the kinetics and mechanism of reduction. Chapter two is an outline of the theory relevant to this study. Chapter three describes the experiments and chapter four outlines of the results and discussion.

The second part (which was the project first started) was aimed at 'Novel syntheses by means of the Kolbe reaction'. This is outlined in chapter five. This study occupied the first year but did not reach any definite conclusion and was terminated; the account is given to complete the record of work carried out.

CHAPTER I CYCLIC VOLTAMMETRY

I INTRODUCTION

The origin of voltammetric methods using solid electrodes may be traced to the classic research of Le Blanc[1]. Following an investigation of the decomposition voltages of acid and base solution Le Blanc studied the hydrolysis of metal ions, working with Nernst at Gottingen in 1897. Salomen[2] used current voltage curves to derive limiting currents.

In 1925, J. Heyrovsky and M. Shikata[3] introduced the polarographic technique which is based on the interpretation of the current potential characteristic exhibited by the dropping mercury electrode (DME). In practice polarograms are almost invariably constructed using linear sweeps of potential, and polarography is probably the most widely used single form of voltammetry. Besides the dropping mercury electrodes (DME), rotating electrodes (RE) or stationary electrodes (SE) is stirred and unstirred solution can also utilized in the determination of current potential curves. Such voltammetric measurements are useful in chemical analysis as was first demonstrated by Laitinen and Kolthoff[4] in 1941.

In conventional polarography and voltammetry the voltage applied to the electrolytic cell is essentially kept constant during the measurement of the current and the measurements are made point by point. Current voltage curves for stationary electrode (SE) can also be recorded by varying continuously the voltage applied to the electrochemical cell as was first shown by Matheson and Nichols[5] in 1938. The fundamentals of voltammetry with continuously changing potential were established by Sevcik[54a] and Randles[55a] for reversi-

ble processes and by Delahay[56a] for irreversible processes.

In the foregoing voltammetric methods the electrolysis current is the measured quantity, and the voltage applied to the electrolytic cell is the variable being controlled. Electrolysis at controlled current, the galvanostatic method is a well established technique, although it has been descreasingly used in recent years. Weber[6] was the first to apply electrolysis at constant current in the verification of Fick's second law for diffusion controlled processes

$$\frac{\partial C}{\partial t} = D \frac{\partial^2 C}{\partial X^2} \qquad 1.1.1.$$

$$i = nDF\left(\frac{\partial C}{\partial X}\right)_{x=0} = \text{constant.}$$

The theory of voltammetry at constant current was developed by Sand[57a] and Karoglanoff[58a] in the early twentieth century and further theoretical advances were recently made by Delahay and his co-workers[59a].

Controlled potential methods are now generally employed and in the last two decades, voltammetric methods have been extended to include irreversible processes. The applications range from inorganic systems in aqueous solution, to organic electrochemical reactions in non-aqueous solvents, and the methods are also widely used in other fields such as in fused salts.

The growth from the 1950's dealing with solid electrodes parallels the rapid increase of the general polarographic literature as cited by Kolthoff and Lingane.[7]

II Theoretical aspects of cyclic voltammetry

Cyclic voltammetry is a particular form of voltammetry that allows one to the scan the potential of the working electrode in the cathodic or anodic direction and to observe peaks in the current due to the reduction or oxidation of the substrates. The potential is usually successively scanned in the cathodic and anodic directions and peaks due to reduction or oxidation of intermediates formed during the forward scan may be observed on the reverse scan. The electrode systems used in cyclic voltammetry include planar platinum disk electrodes, platinum wire electrodes, hanging mercury electrodes (HMDE) and carbon paste electrodes. Other kinds of metals have also been studied.

In cyclic voltammetry the current (both cathodic and anodic segments) is followed during the complete excursions of the applied triangular voltage sweep. The sweep rates can be about the same as in single-sweep peak voltammetry. The instrumentation for cyclic voltammetry generally consists of a controlled potential or three-electrode system[8] with a triangular waveform generator which produces voltage sweep rates ranging from about 10^{-2}V/s to 10^{3}V/s. Voltammograms are recorded on a X-Y recorder for low sweep rates while oscilloscopic recording is used for high sweep rates.

Since cyclic voltammograms are observed at electrodes in unstirred solution and the time interval between the forward and reverse sweeps are relatively short, products of say, a cathodic reduction, are available at and near the electrode surface for reoxidation on the anodic going segment of the cyclic sweep. Ideally, cyclic voltammetry should employ strictly linear diffusion conditions.

The initial scan up to the potential at which the sweep is reversed corresponds to the conditions for the recording of a peak voltammogram. Thus, the equations of peak voltammetry apply to cyclic voltammetry. The current at the peak potential is given by the equation

$$i_p = k n^{3/2} A D^{1/2} C \nu^{1/2} \qquad 1.2.1.$$

or

$$(i_p) = 0.474 (nF)^{3/2} C_A (\nu D)^{1/2} / (RT)^{1/2} \qquad 1.2.2.$$

where,

i_p is the peak current in amperes,

A is the area of the electrode in cm^2,

ν is the scan sweep rate of potential in V/s,

k is the constant called the Ševčik-Randles constant,

D is the diffusion coefficient of the electroactive substance in cm^2/s,

C is the concentration of electroactive substance in mole/litre,

F is the Faraday constant,

R is the Gas constant,

T is the temperature,

The current potential curves (i-E curves) are most commonly called peak polarograms and the techniques have been known as peak voltammetry, peak polarography, or linear sweep chronoamperometry. The curve may be characterized by the peak potential (E_p), or the half peak potential ($E_{p/2}$). The latter is defined as the potential at

which

$$i = i_{p/2} \qquad 1.2.3.$$

Equation 1.2.1 holds for rapid charge-transfer processes that is for reversible reactions.

Matsuda and Ayabe[9] considered the relative rates of charge transfer and mass transfer. For the reversible case they found that simple relations exist between the peak potential E_p, half peak potential $E_{p/2}$ and the conventional half-wave potential $E_{1/2}$ of the dropping mecury electrode (DME), such as at 25°C;

$$E_p = E_{1/2} - \frac{0.029}{n}V \qquad 1.2.4.$$

$$E_{p/2} = E_{1/2} - \frac{0.028}{n}V \qquad 1.2.5.$$

$$\left| E_p - E_{p/2} \right| = \frac{0.057}{n}V \qquad 1.2.6.$$

where,

n is the number of electrons transfered in the electrode reaction.

It can be seen from equation (1.2.6.) that the peak polarogram of a reversible system is sharp.

Equation (1.2.1) may be arranged to give the useful expression

$$i_p / v^{\frac{1}{2}}C = k' \qquad 1.2.7.$$

where,

k' combines all the constants of the previous equation.

Thus for a reversible charge transfer in the absence of

chemical complications the peak current divided by the square root of the voltage sweep rate and by the concentration of the substrate is a constant independent of the sweep rate.

The equation for a totally irreversible system is more complicated. The peak current is expressed by

$$i_p = 3.01 \times 10^5 . n(\alpha n_a)^{\frac{1}{2}} . A . D^{\frac{1}{2}} . V^{\frac{1}{2}} \qquad 1.2.8.$$

where,

n_a is the number of electrons per molecule of reactant in the rate determining step,

α is the transfer coefficient,

and the other terms have the same meaning as in equation (1.2.1.). The value of αn_a can be estimated from the relation.

$$\alpha n_a = \frac{0.048}{E_p - E_{p/2}} V \qquad 1.2.9.$$

In linear sweep voltammetry the observed current density is the sum of a nonfaradaic component i_{nf} and a faradaic component i_f; assuming a priori separation of faradaic and nonfaradaic currents,

$$i = i_{nf} + i_f$$

$$C_d \qquad = Cd(\frac{dE}{dt}) + i_f \qquad 1.2.10.$$

where C_d is the double layer capacitance

In slow sweep voltammetry (i.e. voltage sweep rate < 10^{-2}V/s) however, the nonfaradaic current densities are usually small compared to the faradaic component. At faster sweep rates the nonfaradaic

component may become quite large and strongly influence the shape of the cyclic voltammetric curves.

The faradaic currents have been treated for both reversible and irreversible multiple step electrode processes with diffusion being taken into account on plane electrode[10-16]; spherical electrodes[16,17] and cylindrical electrodes[17].

For a reversible cathodic electron-transfer process of the form

$$O + ne \rightleftharpoons R$$

the faradaic current density can be expressed according to Nicholson and Shain[17], as

$$i_f = i_p + s \qquad 1.2.11.$$

where,

i_p is the current density for a plane electrode,

s is the correction for the case of a spherical electrode.

The faradaic current density on a plane electrode is related to the voltage scan rate (ν) in the cathodic direction by the equation

$$i_p = (nF)^{3/2} C^o(\nu D)^{\frac{1}{2}} E_p/(RT)^{\frac{1}{2}} \qquad 1.2.12.$$

where,

C^o is the bulk concentration of the species O

E_p is the function of the electrode potential,

n is the number of electron transfered,

F, R, D, T are mentioned before.

The spherical correction is s is given by

$$S = nFC^{o}DE_{s}/a_{s} \qquad 1.2.13.$$

where,

E_s is a factor for which numerical values have also been tabulated as a function of potential by Nicholson and Shain[15],

a_s is the radius of the electrode,

The form of the current-voltage curve shown in fig (1.1) for a reversible charge transfer process is controlled principally by the factor E_p which passes through a maxium as the potential is swept in the cathodic direction. The potential E for the maximum current i is

$$E_m = E_{1/2} - \frac{(1.11)RT}{nF} \qquad 1.2.14.$$

where,

E_m is the maximum potential,

The half-wave potential ($E_{1/2}$) of solid electrode polarograms is taken as the potential where $i=i_{L/2}$. For stationary electrodes where peak-shape polarograms are obtained $E_{p/2}$ is a close counterpart of $E_{1/2}$ at a rotated electrode. Half-wave potentials at solid electrodes may not be as accurate as at the dropping mercury electrode (DME) for several reasons. First, lack of reproducibility

of surface conditions gives rise to distortion in the polarogram. Second, the shape of recorded current-voltage curves may vary with the rate of change of applied voltage. On the other hand, if these factors are held invarient, it is possible to obtain reproducibility in $E_{1/2}$ and $E_{p/2}$ measurements of $\pm$ 1-2mV.

The half-wave potential can be evaluated from the current-voltage curve for the reversible case since it occurs at $i=0.852i_m$. Where, i_m is the peak current density.

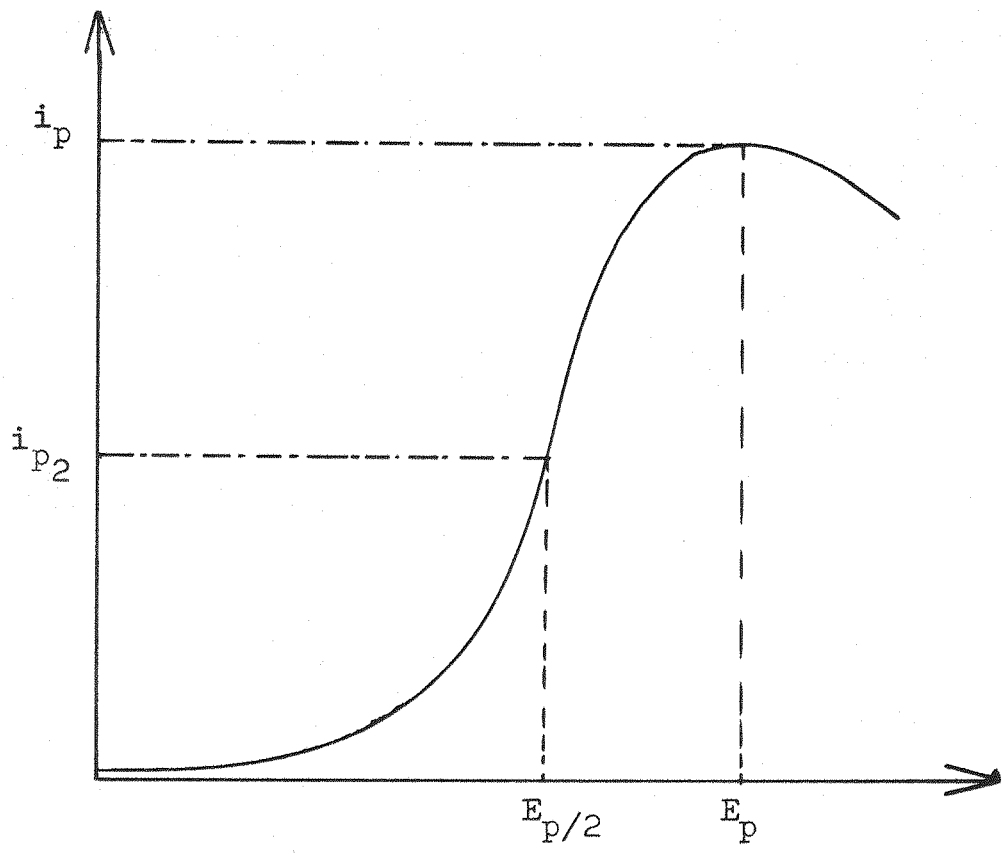

Fig.1 Linear sweep rate voltammetry curve for a reversible charge transfer process.

III The electrochemical reduction of polycyclic aromatic hydrocarbons

The electrochemistry of polycyclic aromatic hydrocarbons in non-aqueous (aprotic) solvents has been the subject of a number of studies[18]. These investigations are of interest because the radical ions which are formed at the electrode may undergo further chemical or electrode reactions.

The first reported polarographic studies of reduction of polycyclic aromatic hydrocarbons were carried out with 75% dioxane-water by Wawzonek et al[19-20]. A clear indication of the nature of the reaction was made by Hoijtink et al[21]. The latter workers used 96% dioxane-water and found that in this solvent of relatively low proton availability polycyclic aromatic hydrocarbon undergo one electron transfer reduction to form the free radical anion;

$$R + e \rightleftharpoons R^-$$

Similar results and conclusions were obtained with anhydrous dimethylformamide (DMF)[22-25] and acetonitrile[26] solvents in which the proton availability is considerably less than that in 96% dioxane. These conclusion drawn originally from the shape and height of the polarographic curves have been confirmed by detection of the radical anion by controlled potential electrolysis[27-28a], a.c. polarography[29-30] and cyclic voltammetry[31-32]. Moreover, the polarographic curves suggest that the electron transfer is diffusion controlled. Kinetics studied by relaxation methods show very fast reaction. Table 1. lists standard rate constants on Hg. The reactions are very fast and at the limit of the techniques bearing in mind particularly the resistance of the media.

Aromatic hydrocarbons undergo further reduction at more

TABLE 1

Experimental information on rates of electrode reactions involving only electron transfer.

System	Electrode	Medium	E_c^o(SCE)	k(cm/s)	α	Ref.
Naphthalene	Hg	DMF/0.1M TBAI/30°	-2.49	1.0	0.56	35
Anthracene	Hg	DMF/0.1M TBAI/25°	-1.95	4.0	-	33
Tetracene	Hg	DMF/0.1M TBAI/30°	-1.58	1.64	0.52	35
Perylene	Hg	DMF/0.1M TBAI/25°	-1.67	4.0	-	33
$\{Anthracene\}^-$	Hg	DMF/0.1M TBAI/25°	-2.55	9.1×10^{-3}	-	33
$\{Perylene\}^-$	Hg	DMF/0.1M TBAI/25°	-2.26	8.7×10^{-3}	-	33
trans-Stilbene	Hg	DMF/0.1M TBAI/30°	-2.15	1.22	0.58	35
Cyclo-octa tetraene	Hg	DMF/0.1M TEAP/25°	-1.62	8.7×10^{-3}	-	36
Azobenzene	Hg	DMF/0.1M TEAP/-	-1.81	0.5	0.37	37

Standard potentials E_c^o are referred to a saturated calomel electrode, except for Azobenzene result which refers to a Ag/Ag^+ electrode in DMF.

TBAI = Bu_4NI

TEAP = Et_4NClO_4

α is the transfer coefficient.

negative potentials. The characteristics of this reduction are much less clear than those of the first electron transfer step. The second wave is about half a volt more negative than the first; the height usually corresponds to that for a 1e transfer and the shape indicates that the reaction is irreversible. Hoijtink and his co-workers have made a study of the kinetics of these processes by a.c. polarography and impedance measurements in DMF[29-30-33]. Peover suggested that the rate of electron transfer to the radical anions may be affected by the potential region in which the transfers occurs, perhaps by the potential dependance of the structure of the electrode double layer.

A wide range of aromatic compounds has been found to show polarographic behaviour very similar to the described for the polycyclic aromatic hydrocarbons. The solvents chiefly employed were DMF and acetonitrile.

In acetonitrile and DMF solution the half wave potentials have been found to shift in a positive direction with change of cation in the order Li > Na > K > Cs indicating stabilisation of the product by ion pairing. If a tetraalkylammonium salt is used as supporting electrolyte, it is possible that the aromatic radical ions are essentially free in this environment, and the formation constants and stoichiometry of the ion pairs with added smaller cations can be obtained from the resulting shifts in half-wave potential.

The aromatic anion radicals or dianions formed initially by the electron transfer process at the electrode have varying degrees of stability depending on their structure and the solvent. Although by polarographic standards many aromatic compounds yield stable anions[25,27], significant rates of reaction may be found on a longer time scale, such as is commonly encountered in a controlled-potential electrolysis. It has recently

been found, however, that when controlled-potential electrolyses are carried out in highly purified solvents such as DMF, the anion radical of 9,10 DPA (9,10 diphenylanthracene), 9,10 DMA (9,10 dimethylanthracene) 9-phenylanthracene, anthracene, chrysene and perylene etc are stable in solution, and the ratio of the peak current of the first cathodic wave to that of the reverse anodic wave $i_{p_c}/i_{p_a} = 1$ [28a]. In cases where the radical anions or dianions are considerably more reactive or, alternatively the solvent is more acidic, the larger rate of proton addition leads to profound changes in the polarographic characteristics of the reduction process. Indeed, the changes that occur in the polarographic behaviour of aromatic compounds on the controlled addition of proton donor to nominally aprotic solvents had led to valuable information on the protonation in electrochemical processes.

It has been noted that for most aromatic hydrocarbons the second wave is irreversible, and this could be due to a low rate of electron transfer or to a coupled chemical reaction of the dianions formed. In 96% dioxane the second wave of anthracene is irreversible owing to proton addition, as shrown by cyclic voltammetry[31]. In polycyclic aromatic hydrocarbons for which protonation of the dianions results in a molecule containing a residual polycyclic system, the effect of protonation can be to increase the height of the second wave, as the residual aromatic system becomes available for further reduction or a further new wave at more negative potentials may appear.

Similar results has been obtained for the reduction of perylene and perylene anion radicals in DMF[34].

CHAPTER II

CHAPTER II

The theory of cyclic voltammetry on planar and spherical electrodes for the case of reversibility at the surface.

INTRODUCTION

The work described in the first part of this thesis is concerned with the development of a new method for measuring the kinetics of fast electron transfer reactions using slow linear sweep voltammetry on micro-electrodes. The underlying concepts are as follows: It is well known that on a planar electrode the mass transfer to the surface is determined by the parameter $\frac{D}{\delta}$ where δ is the boundary layer thickness $\sim 10^{-3}$ cm (in well stirred solutions) and $D \sim 10^{-5}$ cm^2/s. It follows that the heterogeneous rate constants accessible to measurement are limited by this mass transfer coefficient so that k must be $< 10^{-2}$ cm/s. The last 20 years has been seen the development of a large number of relaxation methods which have been designed to measure rate constants in excess of this value. In these methods mass transfer to the surface is determined by the parameter $(\frac{D}{t})^{\frac{1}{2}}$ where t is the duration of the experiment, so that if $t \sim 10^{-5}$ sec. then the measurable rate constants approach $k \sim 1$ cm/s. Relaxation methods have been beset by a number of difficulties, the chief being the fact that the reactance of the double layer capacitance becomes the dominant impedance element at such short times or at high frequencies; adsorption at the electrode and the associated pseudo capacitances also have a serious effect.

In constrast to steady state or relaxation measurements on planar electrodes, mass transfer in the spherical diffusion field surrounding a microelectrode of radius r is determined in the steady state by the parameter $\frac{D}{r}$ so that if $r \sim 10^{-5}$cm then the accessible rate constants $k \sim 1$ cm/s in such a steady state. Previous work has demonstrated these effects ofr the mercurous/ mercury reaction on growing mercury drops in a thin layer cell configuration.[60a] The present work is an attempt to extend these ideas to single solid microelectrodes which might be applicable for a wider variety of reactions. Chapter II covers the relevant theoretical background for planar and spherical electrodes.

I Planar electrode

A very common electrode process of organic molecules is the gain or loss of one electron in a so-called reversible reaction which is written in a general form as

$$O + e \rightleftharpoons R \qquad 2.1.1.$$

An electrochemical reversible reaction is one in which the rates of electron transfer are high compared to diffusion to and from the surface. The concentrations of the species O and R are then governed by thermodynamic considerations and can be determined by use of the Nernst equation.

$$E \simeq E_o + \frac{RT}{F} \ln \frac{C_O}{C_R} \qquad 2.1.2.$$

where,

E_o is the standard potential,

E is the applied potential,

R is the gas constant,

T is the temperature,

C_O and C_R are the concentrations of the species O and R. (More correctly the activities of species O and R should be used.)

Now, consider the effect of changing the potential of a planar electrode upon the concentration of the species O and R close to the electrode surface. The initial potential is E_1, the initial concentrations of O and R are C_O^∞ and C_R^∞ and thus from equation (2.1.2)

$$E_1 \simeq E_o + \frac{RT}{F} \ln \frac{C_O^\infty}{C_R^\infty} \qquad 2.1.3.$$

The potential { E(t) } as a function of time (t) is given by

$$E(t) = E_1 - at \qquad 2..1.4.$$

where,

a is the potential sweep rate.

The concentration of species O and R at any time (t) are C_O and C_R.

Hence, from equation (2.1.2.)

$$E(t) = E_o + \frac{RT}{F} \ln \frac{C_O}{C_R} \qquad 2.1.5.$$

$$E_1 - at = E_o + \frac{RT}{F} \ln \frac{C_O}{C_R} \qquad 2.1.6.$$

Substituting equation (2.1.3.) into equation (2.1.6.) for E_o gives

$$\frac{RT}{F} \ln \frac{C_O^\infty}{C_R^\infty} - at = \frac{RT}{F} \ln \frac{C_O}{C_R} \qquad 2.1.7.$$

or $$\frac{C_O}{C_R} = \frac{C_O^\infty}{C_R^\infty} \exp - \frac{atE}{RT} = k \exp -bt \qquad 2.1.8.$$

In the treatment $\frac{C_O^\infty}{C_R^\infty}$ will be chosen to be large.

Assuming the solution to extend to infinity then the flows of O and R in the X-direction perpendicular to electrode surface are governed by Fick's second law.

$$\frac{\partial C_o}{\partial t} = D_o \frac{\partial^2 C_O}{\partial x^2} \qquad 2.1.9.$$

$$\frac{\partial C_R}{\partial t} = D_R \frac{\partial^2 C_R}{\partial x^2} \qquad 2.1.10.$$

where,

D_O and D_R are the diffusion coefficients of the species O and R.

t is the time,

x is the distance along a line normal to the electrode surface.

and for simplicity it will be assumed that

$$D_O = D_R = D \qquad 2.1.11.$$

The initial conditions are:-

$$C_O = C_O^\infty \qquad 0 < X < \infty \quad t = 0 \qquad 2.1.12.$$

$$C_R = C_R^\infty \qquad 0 < X < \infty \quad t = 0 \qquad 2.1.13.$$

The boundary conditions are:-

$$C_O = C_O^\infty \qquad X = \infty \quad t > 0 \qquad 2.1.14.$$

$$C_R = C_R^\infty \qquad X = \infty \quad t > 0 \qquad 2.1.15.$$

$$-\frac{\partial C_O}{\partial r} = \frac{\partial C_R}{\partial r} \qquad X = 0 \quad t > 0 \qquad 2.1.16.$$

together with equation 2.1.8

One further condition can be derived from equation (2.1.8.) and equation (2.1.16.) by noting that in view of equation (2.1.16.).

$$C_O + C_R = C_O^\infty + C_R^\infty \qquad 2.1.17.$$

So that

$$C_O = \frac{(C_O^\infty + C_R^\infty)k \exp -bt}{1 + k \exp -bt} \qquad 2.1.18.$$

It is convenient to solve equation (2.1.9.), (2.1.10.) and (2.1.18.) by using the Laplace transformation. Equation (2.1.9.) and (2.1.10.) thus become

$$\frac{d^2\bar{C}_O}{dx^2} - q^2\bar{C}_O + \frac{C_O^\infty}{D} = 0 \qquad 2.1.19.$$

$$\frac{d^2\bar{C}_R}{dx^2} - q^2\bar{C}_R + \frac{C_R^\infty}{D} = 0 \qquad 2.1.20.$$

where,

$$q^2 = \frac{S}{D}$$

and S is the variable of the Laplace transformation.

Rewriting equation (2.1.18.) as

$$C_O = (C_O^\infty + C_R^\infty)k \exp -bt(1+k \exp -bt)^{-1}$$

$$\therefore C_O = (C_O^\infty + C_R^\infty)k_\infty \exp -bt(1-k \exp -bt + k^2 \exp -2bt \text{ ------})$$

$$= (C_O^\infty + C_R^\infty)\sum_{n=1}(-1)^{n+1}k^n \exp -nbt \qquad 2.1.22.$$

this transforms to

$$\overline{C}_O = (C_O^\infty + C_R^\infty)\sum_{n=1}^{\infty}\frac{(-1)^{n+1}k^n}{S + nb} \qquad 2.1.23.$$

at $x = 0$

The solution of equation (2.1.19.) is

$$\overline{C}_O = \frac{C_O^\infty}{S} + G \exp qx + H \exp -qx \qquad 2.1.24.$$

where,

G and H are determined from the boundary conditions. The solution of equation (2.1.20.) will not be necessary in view of the complete specification of C_O at $x = 0$. Equation (2.1.14.) shows that

$$G = 0 \qquad 2.1.25.$$

Equation (2.1.24.) and (2.1.23.) at $x = 0$ gives

$$\frac{C_O^\infty}{G} + H = (C_O^\infty + C_R^\infty)\sum_{n=1}^{\infty}\frac{(-1)^{n+1}k^n}{S + nb} \qquad 2.1.26.$$

$$\text{ie} \quad \overline{C}_O = \frac{C_O^\infty}{S} - \frac{C_R^\infty}{S}\exp -qx + (C_O^\infty + C_R^\infty)\sum_{n=1}^{\infty}\frac{(-1)^{n+1}k^n \exp -qx}{S + nb} \qquad 2.1.27.$$

The current i is given by

$$\overline{i} = DF\left(\frac{d\overline{C}_O}{dx}\right)_{x = 0} \qquad 2.1.28.$$

which on transformation gives

$$i = DF\left(\frac{dC_O}{dx}\right)_{x = 0}$$

$$= \frac{D^{\frac{1}{2}}FC_O}{S^{\frac{1}{2}}} + D^{\frac{1}{2}}F(C_O + C_R)\sum_{n=1}^{\infty}\frac{(-1)^n k^n s^{\frac{1}{2}}}{S + nb} \qquad 2.1.29.$$

which inverts to give

$$i = \frac{D^{\frac{1}{2}}FC_O}{(\ t)^{\frac{1}{2}}} + D^{\frac{1}{2}}F(\ C_O + C_R\ )\sum_{n=1}^{\infty}\frac{(-1)^n k^n}{(\ t)^{\frac{1}{2}}}$$

$$-2D^{\frac{1}{2}}F(\ C_O + C_R\ )\sum_{n=1}^{\infty}\frac{(-1)^n k^n (nb)^{\frac{1}{2}}}{\frac{1}{2}} \exp -nbt$$

$$\times \int_0^{(nbt)^{\frac{1}{2}}} \exp \lambda^2 d\lambda \qquad 2.1.30.$$

where,

λ is a dummy variable,

The second term on R.H.S. of equation (2.1.30.) can be summed as

$$-D^{\frac{1}{2}}F(C_O+C_R)(\frac{k}{k+1})\frac{1}{(\pi t)^{\frac{1}{2}}} = \frac{-D^{\frac{1}{2}}FC_O}{(\pi t)^{\frac{1}{2}}} \qquad 2.1.31.$$

Thus,

$$i = \frac{2D^{\frac{1}{2}}F(C_O+C_R)}{\frac{1}{2}}\sum_{n=1}^{\infty}(-1)^{n+1}k^n(nb)^{\frac{1}{2}}\exp -nbt$$

$$\times \int_0^{(nbt)^{\frac{1}{2}}} \exp \lambda^2 d\lambda$$

The current will be a maximum. When $\frac{di}{dt} = 0$

$$\text{ie} \quad \sum_{n=1}^{\infty} (-1)^n k^n (nb)^{1\frac{1}{2}} \exp -nbt \int_0^{(nbt)^{\frac{1}{2}}} \exp \lambda^2 d\lambda$$

$$+ \sum_{n=1}^{\infty} \frac{(-1)^{n+1} k^n (nb)}{2t^{\frac{1}{2}}} = 0 \qquad 2.1.33.$$

Clearly this is a function of a dimensionless time

$$T = bt \qquad 2.1.33.$$

Thus, the maximum will occur a fixed value of bt. The solution of equation (2.1.33.) is evidently tedious.

IIA The theory for reversible electrochemical processes on spherical electrodes

The case when the electrochemical reaction, equation (2.1.1.), occurs at spherical electrode will now be considered. The distance r will be measured radially from centre of the electrode (radius r_o). The flux of O and R are now given by

$$\frac{\partial C_O}{\partial t} = D\frac{\partial^2 C_O}{\partial r^2} + \frac{2D}{r}\frac{\partial C_O}{\partial r} \qquad 2.2.1.$$

$$\frac{\partial C_R}{\partial t} = D\frac{\partial^2 C_R}{\partial r^2} + \frac{2D}{r}\frac{\partial C_R}{\partial r} \qquad 2.2.2.$$

The initial conditions are:-

$$C_O = C_O^\infty \qquad r_o < r < \infty \qquad t = 0 \qquad 2.2.3.$$

$$C_R = C_R^\infty \qquad r_o \quad r < \infty \qquad t = 0 \qquad 2.2.4.$$

The boundary conditions are:-

$$C_O = C_O^\infty \qquad r = \infty \qquad t > 0 \qquad 2.2.5.$$

$$C_R = C_R^\infty \qquad r = \infty \qquad t > 0 \qquad 2.2.6.$$

and

$$C_O = (C_O^\infty + C_R^\infty)\sum_{n=1}^{\infty}(-1)^{n+1}k^n \exp -nbt \qquad 2.2.7.$$

The Laplace transformation of equation (2.2.1.) is

$$\frac{d^2\overline{C}_O}{dr^2} + \frac{2}{r}\frac{d\overline{C}_O}{dr} - q^2\overline{C}_O + \frac{C_O^\infty}{D} = 0 \qquad 2.2.8.$$

and if

$$\overline{V}_o = r\overline{C}_O \qquad 2.2.9.$$

$$\frac{d^2\overline{V}_o}{dr^2} - q^2\overline{V}_o + \frac{rC_O^\infty}{D} = 0 \qquad 2.2.10.$$

The general solution is

$$\overline{V}_o = M \exp qr + N \exp -qr + \frac{rC_O^\infty}{S} \qquad 2.2.11.$$

or

$$\overline{C}_O = M \exp qr + \frac{N}{r} \exp -qr + \frac{C_O^\infty}{S} \qquad 2.2.12.$$

As for the equation (2.1.25.) of the planar electrode

$$M = 0 \qquad 2.2.13.$$

and at $r = r_o$

$$\frac{N}{r_o}\exp -qr_o + \frac{C_O^\infty}{S} = (C_O^\infty + C_R^\infty)\sum_{n=1}^{\infty}\frac{(-1)^{n+1}k^n}{S + nb} \qquad 2.2.14.$$

or

$$\overline{C}_O = \frac{C_O^\infty}{S} - \frac{C_O^\infty r_o}{Sr} \exp -q(r-r_o) + (C_O^\infty+C_R^\infty)\frac{r_o}{r}\exp -q(r-r_o)$$
$$\times \sum_{n=1}^{\infty}\frac{(-1)^{n+1}k^n}{S + nb} \qquad 2.2.15.$$

The current density is given by

$$\bar{i} = FD\left(\frac{d\bar{C}_O}{dr}\right)_{r=r_o}$$

$$= \frac{FDC_O^\infty}{Sr_o} + \frac{FDC_O^\infty q_o}{S} - \frac{FD(C_O^\infty+C_R^\infty)}{r_o}\sum_{n=1}^{\infty}\frac{(-1)^{n+1}k^n}{S+nb}$$

$$- DF(C_O^\infty+C_R^\infty)q_o\sum_{n=1}^{\infty}\frac{(-1)^{n+1}k^n}{S+nb} \qquad 2.2.16.$$

If we compare this to the transform of the current on a planar electrode, equation (2.1.29.) we see that on the spherical electrode we have the additional current with transform

$$\bar{i} = \frac{FDC_O^\infty}{Sr_o} + \frac{FD(C_O^\infty+C_R^\infty)}{r_o}\sum_{n=1}^{\infty}\frac{(-1)^n k^n}{S+nb} \qquad 2.2.17.$$

which inverts to

$$i = \frac{FDC_O^\infty}{r_o} + \frac{FD(C_O^\infty+C_R^\infty)}{r_o}\sum_{n=1}^{\infty}(-1)^n k^n \exp -nbt$$

$$= \frac{FDC_O^\infty}{r_o} - \frac{FD(C_O^\infty+C_R^\infty)}{r_o}\,\frac{k \exp -bt}{1+k \exp -bt} \qquad 2.2.18.$$

Simplified equation (2.2.18.) is

$$i = i_D - \frac{FD(C_O^\infty+C_R^\infty)}{r_o}\,\frac{k \exp -bt}{1+k \exp -bt}$$

$$= i_D - i_D\left(\frac{k \exp -bt}{1+k \exp -bt}\right)$$

Since $C_O^\infty \gg C_R^\infty$.

Therefore

$$i_D - i = i_D\left(\frac{k \exp -bt}{1+k\exp -bt}\right)$$

$$\frac{i_D-i}{i_D} = \frac{k\exp -bt}{1+k\exp -bt}$$

$$\frac{i_D}{i_D-i} = 1 + \frac{1}{k}\exp -bt$$

$$\frac{i_D}{i_D-i} - 1 = \frac{1}{k}\exp -bt$$

$$\frac{i_D}{i_D-i} = \frac{1}{k}\exp -bt \qquad 2.2.19.$$

or

$$\frac{i_D-i}{i} = k\exp -bt \qquad 2.2.20.$$

Which is the steady state current. Thus, if the total current is i_t and we subtract an appropriate amount as if the spherical electrode were planar, i_p, then, the difference must follow equation (2.2.18.) and we can treat the data according to equation (2.2.19.) or (2.2.20.). Alternatively, if it is assumed that $i_p \propto \nu^{\frac{1}{2}}$ in the whole range then we can plot i_t against $\nu^{\frac{1}{2}}$ at each potential. This should give a set of lines the intercepts following the reversible wave, equation (2.2.18.). Of course at sufficiently small ν the total current will follow equation (2.2.18.)

III Irreversible reactions in the steady state

In the case of irreversible reaction we will therefore not introduce the time since the transient has been assumed to be extraploted out.

The boundary conditions at $r = r_o$, may be written directly as

$$D\left(\frac{\partial C_O}{\partial r}\right)_{r=r_o} = \vec{k}(C_O)_{r=r_o}\exp\frac{-\alpha FE}{RT} - \overleftarrow{k}(C_R)_{r=r_o}\exp\frac{(1-\alpha)FE}{RT} \qquad 2.3.1.$$

where,

E is the potential with respect to a reference electrode,

$\vec{k}$ and $\overleftarrow{k}$ are the values of the forward and backward rate constants at E = 0.

Similarly,

$$-D\left(\frac{\partial C_R}{\partial r}\right)_{r=r_o} = \vec{k}(C_O)_{r=r_o}\exp\frac{-\alpha FE}{RT} - \overleftarrow{k}(C_R)_{r=r_o}\exp\frac{(1-\alpha)FE}{RT} \qquad 2.3.2.$$

and

$$D\left(\frac{\partial C_O}{\partial r}\right)_{r=r_o} = -D\left(\frac{\partial C_R}{\partial r}\right)_{r=r_o} \qquad 2.3.3.$$

At $r = \infty$

$$C_O = C_O^{\infty} \qquad 2.3.4.$$

and we assume

$$C_R = 0 \qquad 2.3.5.$$

Equation (2.3.5.) is the simplest defined, limiting value of C_R which can be assumed. Note that there can be no equilibrium condition of equation (2.3.1.) and (2.3.2.). If there were a defined

finite value of C_R, C_R^∞ then there would be such a condition given by

$$\vec{k}C_O^\infty \exp\frac{-\alpha FE_r}{RT} = \overleftarrow{k}C_R^\infty \exp\frac{(1-\alpha)FE_r}{RT} \qquad 2.3.6.$$

where,

E_r is the reversible potential,

Hence,

$$\exp\frac{FE_r}{RT} = \frac{\vec{k}C_O^\infty}{\overleftarrow{k}C_R} \qquad 2.3.7.$$

or,

$$E_r = \frac{RT}{F}\ln\frac{\vec{k}}{\overleftarrow{k}} + \frac{RT}{F}\ln\frac{C_O^\infty}{C_O^\infty}$$

$$= E^\theta + \frac{RT}{F}\ln\frac{C_O^\infty}{C_R^\infty} \qquad 2.3.8.$$

where,

E_r^θ is the standard reversible potential.

We now let the standard potential be the reference point, i.e. we measure E with respect to E_r^θ then

$$\vec{k}C_O^\infty\left(\frac{C_R^\infty}{C_O^\infty}\right)^\alpha \exp\frac{-\alpha FE_r^\theta}{RT} = \overleftarrow{k}C_R^\infty\left(\frac{C_O^\infty}{C_R^\infty}\right)^{1-\alpha} \exp\frac{(1-\alpha)FE_r^\theta}{RT}$$

ie

$$\vec{k}(C_O^\infty)^{(1-\alpha)}(C_R^\infty) \exp\frac{-\alpha FE_r^\theta}{RT} = \overleftarrow{k}(C_O^\infty)^{(1-\alpha)}(C_O^\infty) \exp\frac{(1-\alpha)FE_r^\theta}{RT}$$

$$= k_o(C_O^\infty)^{(1-\alpha)}(C_R^\infty)^\alpha \qquad 2.3.9.$$

where,

k_o is the rate constant of the forward and backward reactions at standard reversible potential. k_o is independent of the concentrations C_O and C_R and as well as of the potential scales and is the only constant of theoretical significance.

We therefore define all potentials with respect to E_r^{θ} and write equation (2.3.1.) and equation (2.3.2.) as

$$D\left(\frac{dC_O}{dr}\right) k_o C_O \exp\frac{-\alpha FE}{RT} - k_o C_R \exp\frac{(1-\alpha)FE}{RT} \qquad 2.3.10.$$

$$-D\left(\frac{dC_R}{dr}\right) = k_o C_O \exp\frac{-\alpha FE}{RT} - k_o C_R \exp\frac{(1-\alpha)FE}{RT} \qquad 2.3.11.$$

We solve for diffusion in the steady state

$$D\frac{d^2C_O}{dr^2} + \frac{2D}{r}\frac{dC_O}{dr} = 0 \qquad 2.3.12.$$

$$D\frac{d^2C_R}{dr^2} + \frac{2D}{r}\frac{dC_R}{dr} = 0 \qquad 2.3.13.$$

giving,

$$C_O = \frac{A}{r} + B$$

$$= \frac{A}{r} + C_O^{\infty} \qquad 2.3.14.$$

and,

$$C_R = \frac{X}{r} + Y$$

$$= \frac{X}{r} \quad \text{(using 2.3.5.)} \qquad 2.3.15.$$

Then, using equation (2.3.4.) and (2.3.7.),

Since

$$\frac{dC_O}{dr} = -\frac{dC_R}{dr} \quad \text{at } r = r_o \qquad 2.3.17.$$

$$A = -X \qquad 2.3.18.$$

using equation (2.3.8.)

$$-\frac{DA}{r_o^2} = k_o\left(\frac{A}{r_o} + C_O^{\infty}\right)\exp\frac{-\alpha FE}{RT} + k_o\frac{A}{r_o}\exp\frac{(1-\alpha)FE}{RT} \qquad 2.3.18.$$

or

$$\frac{A}{r_o^2}\left\{D+k_o r_o\left[\exp\frac{-FE}{RT}+\exp\frac{(1-\alpha)FE}{RT}\right]\right\}=k_o C_O \exp\frac{-\alpha FE}{RT}$$

2.3.19.

or

$$A=\frac{-k_o r_o^2 C_O \exp\frac{-\alpha FE}{RT}}{Dk_o r_o \exp\frac{-\alpha FE}{RT}\left(1+\exp\frac{FE}{RT}\right)}$$

2.3.20.

We note the simplification produced by using k_o and using $C_R = 0$ at $r = \infty$

$$\therefore i=\frac{FDk_o C_O^{\infty}\exp\frac{-\alpha FE}{RT}}{D+k_o r_o \exp\frac{-\alpha FE}{RT}\left(1+\exp\frac{FE}{RT}\right)}$$

2.3.21.

$$\frac{1}{i}=\frac{1}{Fk_o C_O^{\infty}\exp\frac{-\alpha FE}{RT}}+\frac{r_o\left(1+\exp\frac{FE}{RT}\right)}{FDC_O^{\infty}}$$

2.3.22.

We note that as potential gets larger and negative $\exp\frac{FE}{RT} \rightarrow 0$

$$\therefore \frac{1}{Fk_o C_O^{\infty}\exp\frac{-\alpha FE}{RT}} \longrightarrow 0$$

and,

$$\frac{1}{i} \longrightarrow \frac{r_o}{FDC_O^{\infty}} = \frac{1}{i}$$

2.3.23.

If $k_o r_o >> D$, then

$$\frac{1}{i} \simeq \frac{r_o}{FDC_O} + \frac{r_o}{FDC_O} \exp\frac{FE}{RT} \qquad 2.3.24.$$

or,

$$\frac{1}{i} - \frac{1}{i_D} = \frac{1}{i_D} \exp\frac{FE}{RT} \qquad 2.3.25.$$

or,

$$\frac{i_D - i}{i_D} = \exp\frac{FE}{RT} \qquad 2.3.26.$$

i.e. diffusion control as before, equation (2.2.20.).

If $k_o r_o << D$, then over the whole negative range of potential

$$i \simeq \frac{FDk_o C_O^\infty \exp\frac{-\alpha FE}{RT}}{D + k_o r_o \exp\frac{-\alpha FE}{RT}} \qquad 2.3.27.$$

$$\therefore \frac{1}{i} = \frac{1}{Fk_o C_O^\infty \exp\frac{-\alpha FE}{RT}} + \frac{r_o}{FDC_O^\infty} \qquad 2.3.28.$$

or,

$$\frac{i.i_D}{i_D - i} = Fk_o C_O^\infty \exp\frac{-\alpha FE}{RT} \qquad 2.3.29.$$

Which is the irreversible case. However, it is clear that we can not make this approximation at potentials positive to E_r^θ. To obtain a generally valid expression we rewrite equation (2.3.22.) as

$$\frac{1}{i} - \frac{(1+\exp\frac{FE}{RT})}{i_D} = \frac{1}{Fk_o C_O^\infty \exp\frac{-\alpha FE}{RT}} = \frac{i_D - i(1+\exp\frac{FE}{RT})}{i_D.i}$$

2.3.30.

or

$$\frac{i_D \cdot i}{i_D - i(1+\exp\frac{FE}{RT})} = Fk_o C_O^\infty \exp\frac{-\alpha FE}{RT} \qquad 2.3.31.$$

At first sight there is an inconsistency to equation (2.3.31.) as one might expect that $i\{ 1 + \exp \frac{FE}{RT} \} > i_d$ at large positive potentials. However equation (2.3.31.) and (2.3.22.) shows that this can not be so. In fact at positive potential

$$i \simeq \frac{FDC_O^\infty}{r_o} \exp\frac{-FE}{RT}$$

$$= i_D \exp\frac{-FE}{RT} \qquad 2.3.32.$$

Which is expected for diffusion control. Equation (2.3.32.) is as expected when compared to equation (2.3.26.).

The most general form is equation (2.3.30.). Examination of equation (2.3.21.) shows that effects of k_o will be readily detectable provided

$$2k_o r_o \leqslant D \qquad 2.3.33.$$

ie $$k_o \leqslant \frac{D}{2r_o} \qquad 2.3.34.$$

i.e. the 'rate constant' for mass transfer is high compared to that of the surface reaction. Equation (2.3.34.) shows that the rate of mass transfer can be enhanced by reducing r. If r can be made sufficiently small then it should be possible to measure standard rate constants for fast reactions using steady state methods (slow voltammetric sweeps) rather then by relaxation techniques.

CHAPTER III

CHAPTER III

EXPERIMENTAL AND TECHNIQUES

I. SOLVENT DMF (Dimethylformamide)

Even the best grade of DMF available commercially contains electroactive impurities. It is however able to dissolve a wide range of ionic and covalent chemicals, and has the following useful properties:- wide liquid range, thermal stability and high polarity. A summary of the physical properties of DMF is shown in Table 2. Since it is hygroscopic, precautions must be taken to minimize exposure to atmospheric moisture. The commercial product has an unpleasant odour of amine due to moisture absorption and subsequent slight hydrolysis to dimethylamine. Philipp et al[38] and Tury'an et al[39] have suggested that, as a result of hydrolysis, formic acid (HCOOH) is also present in solution; while Moskalyk et al[40] have reported formic acid (HCOOH) as the only impurity in DMF. In addition DMF as received also contains water. Oehme[41] has proposed that photolytic decomposition is a source of impurities in DMF, dimethylamine $\{(CH_3)_2NH\}$ and formaldehyde (HCHO) being the products. Deal et al[42] have further widened the list to include formamide ($HCONH_2$) and N-methylformamide ($HCONHCH_3$) for commerical grades of DMF together with their hydrolysis products.

Ample evidence has been accumulated to show that DMF is unstable in the presence of acidic and basic materials. Thomas et al[43], Moskalyk

et al[41] reported its instability under both of these conditions while the observations of Allen et al[44] and Deal et al[42] are restricted to the behaviour of DMF in basic media. Brunel et al[45] have recently reported that aqueous DMF solutions are unstable in the presence of the hydroxyl ion, with formate ion and dimethylamine $\{(CH_3)_2NH\}$ being the products of decomposition.

DMF decomposes slightly at its normal boiling point, resulting in the formation of carbon monoxide (CO) and dimethylamine $\{(CH_3)_2NH\}$[41,43] ; it therefore must be distilled at reduced pressure. Distilled DMF has most of the properties required of a solvent to be used in electron transfer reactions and it may be used over a wide span of potential. Butler[46] has cited the findings of others who recommend that distillation must be carried out at pressures less than 1 mm of Hg to avoid the thermal decomposition of the formamide ($HCONH_2$). Thomas et al[43] have studied a number of purification methods and found that DMF placed over solid potassium hydroxide (KOH) and calcium hydride (CaH_2) at room temperatures, even for a few hours, caused decomposition giving a "considerable amount" of dimethylamine $\{(CH_3)_2NH\}$ as a product. However, we can conclude from the work of Zuagg et al[47] that the dimethylamine $\{(CH_3)_2NH\}$ formed would be removed during the distillation procedures from the following evidence to be found in their paper. Their purification procedure consisted of shaking benzene (C_6H_6) and dry DMF with phosphorus pentoxide (P_2O_5), decanting the liquid and shaking with potassium hydroxide (KOH) pellets and then distilling under reduced pressure. Now, according to Thomas et al[43] findings, dimethylamine $\{(CH_3)_2NH\}$ would be formed, yet from the analysis of the purif-

ied DMF Zuagg reported no titratable acidic impurities and less than 7×10^{-6} M of dimethylamine to the present. Consequently, calcium hydride (CaH_2) and potassium hydroxide (KOH) can be used to remove formic acid (HCOOH) and water from DMF. From the work of Ritchie et al[48] we can also conclude, as from the work of Zuagg et al[47], that the use of phosphorus pentoxide (P_2O_5) as a purifying agent is not detrimental when the utilization of this reagent is examined from the point of view of the final DMF obtained. Ritchie et al[48] dried DMF with molecular sieves and distilled the DMF at reduced pressure over phosphorus pentoxide (P_2O_5). The product obtained contains less than 5×10^{-6} M of acidic and basic impurities. Thomas et al[43] reasoned that simple vacuum distillation will not remove water from DMF. Their proposal has since been confirmed by the work of Susarev[49] and Ivanova et al[50] who found that for various DMF/H_2O mixtures, distilled under varying pressures, the distillate always contained both components. Hence, we can conclude that water must be removed prior to distillation.

In the case of DMF, upon the basis of this review to date, there appears to be doubt as to which general purification procedures are best; whether, for example, to remove water and other impurities with acidic and or basic reagents or to use molecular sieves and anhydrous cupric sulphate ($CuSO_4$) thus lessening the risk of decomposition of DMF. Consequently it was decided to use the following methods.

The first method: B.D.H. reagent DMF was dried by phosphorus pentoxide (P_2O_5) for several hours with intermittent shaking, followed by fractional distillation while bubbling absolutely dry

nitrogen gas through the liquid. The initial fraction of the distillate was discarded, the middle portion collected and redistilled; this distillate was dried by calcium hydride (CaH_2) and, on further distillation also the middle cut was again collected.

In second method adopted DMF was treated with anhydrous cupric sulphate ($CuSO_4$) prepared by heating B.D.H. A.R. grade cupric sulphate in an oven at 160°C. After standing, with intermittent shaking over the cupric sulphate for ≈ 1 week, the DMF was fractionally distilled under the nitrogen gas bubbling, the initial and the final fractions being rejected. The middle portion was dried with calcium hydride (CaH_2) and redistilled. The distillate was then stored over B.D.H. 4A molecular sieve for two days. A fresh batch of sieve was used for each distillation.

TABLE 2

Summary of DMF physical properties[52]

DMF (dimethylformamide)	$HCON(CH_3)_2$
appearance	colourless, mobile liquid
molecular weight	73.09
boiling point, 760 Torr	153°C
freezing point, 760 Torr	-61°C
specific gravity 25°C / 4°C	0.944
refractive index n_D^{25}	1.4269, 1.4305[53]
vapour pressure, 25°C	3.7 Torr
viscosity, 25°C	0.802 cp
surface tension, 25°C	35.2 dyne/cm
thermal conductivity, 23.5°C	440 cal/sec.cm.°C
dielectric constant, 25°C	36.7
dipole moment, 20°C	3.82 Debye
ionization constant, 20°C	10^{-18}

II SUPPORTING ELECTROLYTE

Several factors determine the choice of supporting electrolyte; these include solubility and electrochemical and chemical inertness. Many nonaqueous solvents are relatively ineffective in dissolving inorganic salts. However, organic salts are often sufficiently soluble. It is especially important for polarography and voltammetry and at least desirable for macro-electrolyses that the supporting electrolyte should be unreactive in the potential region of interest. Aliphatic quaternary ammonium salts meet these criteria especially well. For most organic solvents it is necessary to use at least two-carbon alkyl subsitutents, i.e tetraethylammonium salts Et_4N^+. The most commonly used quaternary ammonium salts include tetrabutylammonium perchlorate Bu_4NClO_4, tetraethylammonium tetrafluoroborate Et_4NBF_4.

Tetraethylammonium tetrafluoroborate Et_4NBF_4 was prepared by mixing hot aqueous solutions of sodium tetrafluoroborate (from B.D. H.) and tetraethylammonium bromide (from Eastman-Kodak). The minium quantity of distilled water was used and the sodium salt solution was filtered before use. On cooling, while crystals of tetra-ethylammonium tetrafluoroborate formed which were filtered off under water-pump suction and recrystallized from distilled water two times until a test with acidic silver nitrate solution no longer showed the presence of bromide ion. Then the product was dried in a vacuum oven at 80°C for at least 48 hours and stored in a dessicator over silica gel.

$$Et_4N^+Br + Na^+BF_4^- \xrightarrow{H_2O} \underset{\text{(white crystal)}}{Et_4NBF_4\downarrow} + NaBr$$

III ORGANIC CHEMICALS

All the experimental chemicals used in the investigation of electron transfer reactions were supplied from Koch-Light laboratories Ltd. They were puriss scintillation grade and were used without further purification. They were stored in a dark cool place. The chemicals used were:-

1. Anthracene $C_{14}H_{10}$, 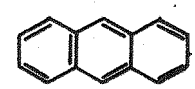 m.w. = 178.23
2. 9-phenylanthracene $C_{20}H_{14}$, 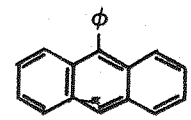 m.w. = 254.33
3. 9,10-diphenylanthracene $C_{26}H_{18}$, 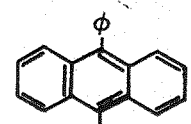 m.w. = 330.43
4. 9,10-dimethylanthracene $C_{16}H_{14}$, 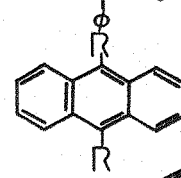 m.w. = 206
5. Chrysene $C_{18}H_{12}$, 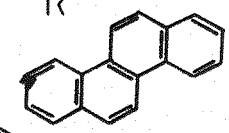 m.w. = 228
6. Perylene $C_{20}H_{12}$ 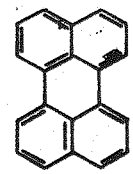 m.w. = 252

Where R = CH_3-

IV GAS TRAIN

Before electrolysis most of the dissolved exygen which is reduced in the potential range of interest and any other electroactive gases were removed by bubbling an inert gas through the solution. It is advisable, especially for small scale work in nonaqueous solvents, such as DMF; to saturate the gas with the solvent before it is introduced into the cell. The inert gas nitrogen or argon as obtained commerically was insufficiently pure. Previously, nitrogen has been purified by bubbling it through solution of Cr(II) or V(II) salts or a Fieser solution. In the work reported in this thesis the nitrogen gas (from B.O.C. gas company) was passed through a mixture of calcium chloride with potassium hydroxide, phosphorus pentoxide and sodium hydroxide with calcium chloride before being led to the dry box used in the experiments.

V ELECTRONIC EQUIPMENT

All electro-chemical experiments on conventional electrodes reported in this thesis were carried out using Chemical Electronics equipment. Generally a 140V/2A valve potentiostat, which has a response time of 1μ sec was used for the experiments which involved varying potential profiles. A chemical electronics waveform generator, type RB1 provided the linear sweep programmes for cyclic voltammetry. Cyclic voltammograms were recorded with sweep rates from 5×10^{-4}V/s to 10^{-1}V/s. A Telequipment oscilloscope type 1210A and a Kodak oscilloscope camera or a Bryans X-Y recorder 26000 A4 were used for recordering current-time transients. The arrangement of the electronic equipments for cyclic voltammetry with Pt-electrodes is shown in fig.4.

The other experiments on indium and lead micro-electrodes were made by applying the voltage output from the waveform generator directly to a two-electrode cell since the currents flowing were sufficiently small for the counter electrode to remain unpolarised and for ohmic loses to be negligible. The currents were measured by using a current follower (D.C. multimeter type TM 9B, Levell Electronic Co.,) the appropriate cell electrode being a virtual earth. The output from the current follower was again recorded on a Bryans X-Y recorder. The system was capable of recording currents down to 1 pA full scale deflection. Appropriate bias potentials were applied in series with the output from the pulse generator; these were derived from a potentiometer with a floating battery supply stabilised by a Zener diode. The circuit lay out is shown in fig.5

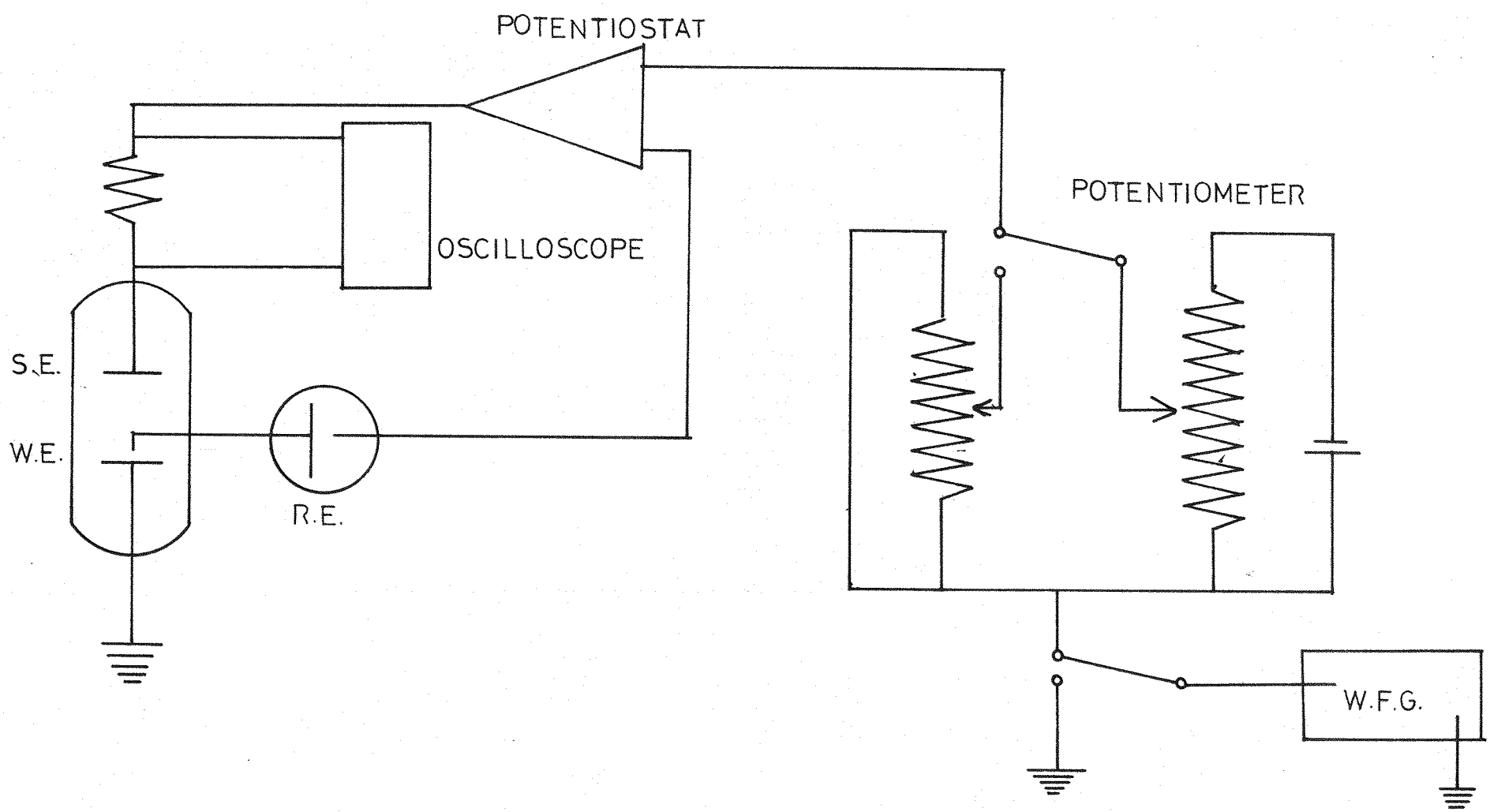

FIG. 4 CIRCUIT DIAGRAM OF A POTENTIOSTAT

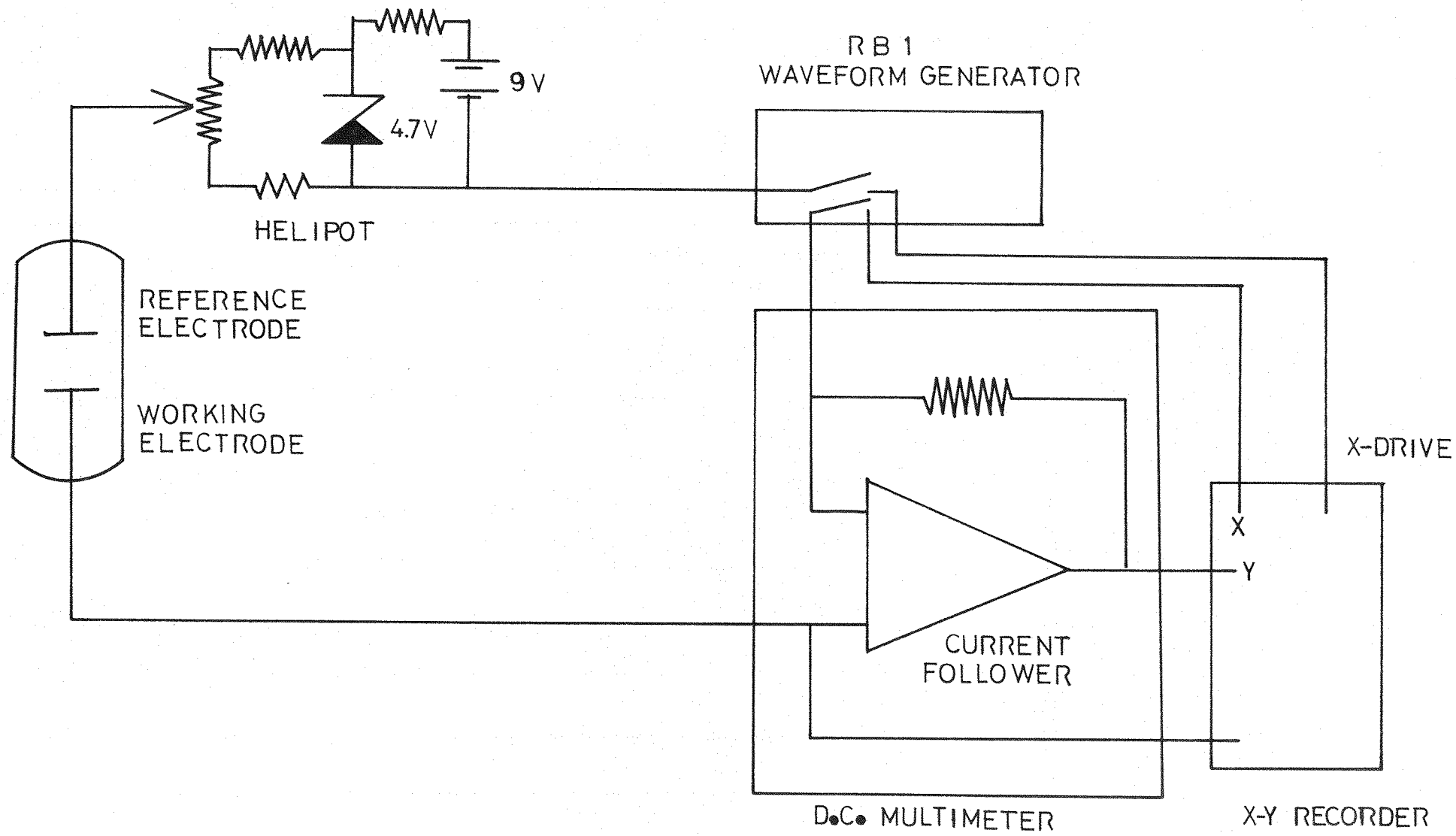
9 V
4.7V
HELIPOT
RB 1
WAVEFORM GENERATOR
REFERENCE
ELECTRODE
WORKING
ELECTRODE
X-DRIVE
X
Y
CURRENT
FOLLOWER
D.C. MULTIMETER
X-Y RECORDER

FIG. 5

VI ELECTROLYTIC CELLS

All experiments were carried out either with three compartment cells or two compartment cells. A special design for cyclic voltammetry is shown in fig.2. The anode and cathode were not separated but arranged as shown; the cell was fitted with a horizontal Luggin capillary and tap as well as a bubbler. All cells were constructed of Pyrex glass care being taken to minimize the volume; the electrode holders were inserted in the usual way through glass joints.

A special cell was designed for measurements on the indium (In) micro-elelctrodes. This cell had two compartments separated by a NO. 4 sinter glass frit. A sleeve joint connected to the working electrode compartment to fit the micro-elelctrode. A gas inlet and bubbler were also attached. The cell design is shown in fig.3.

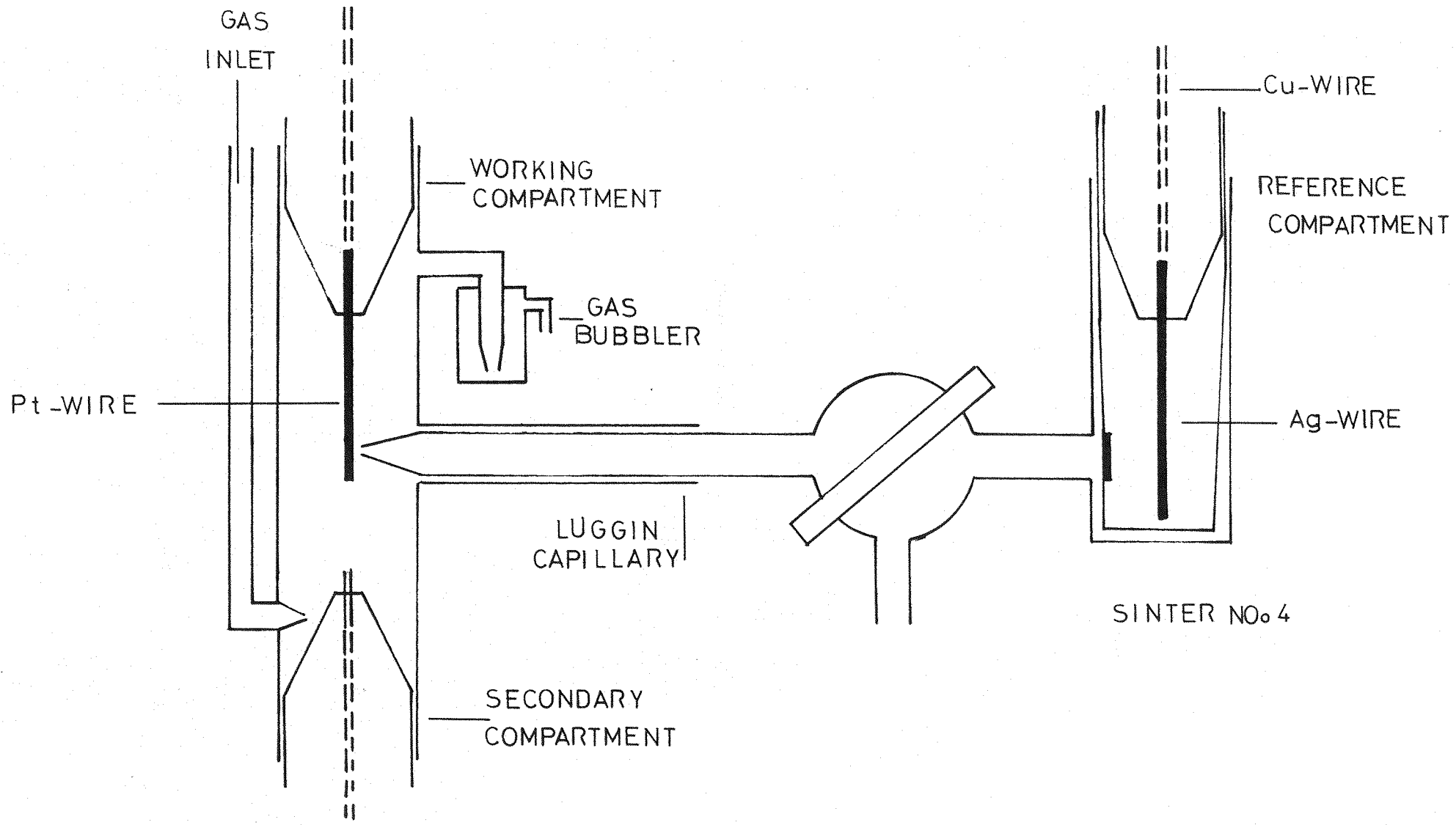

FIG. 2 ELECTROLYSIS CELL

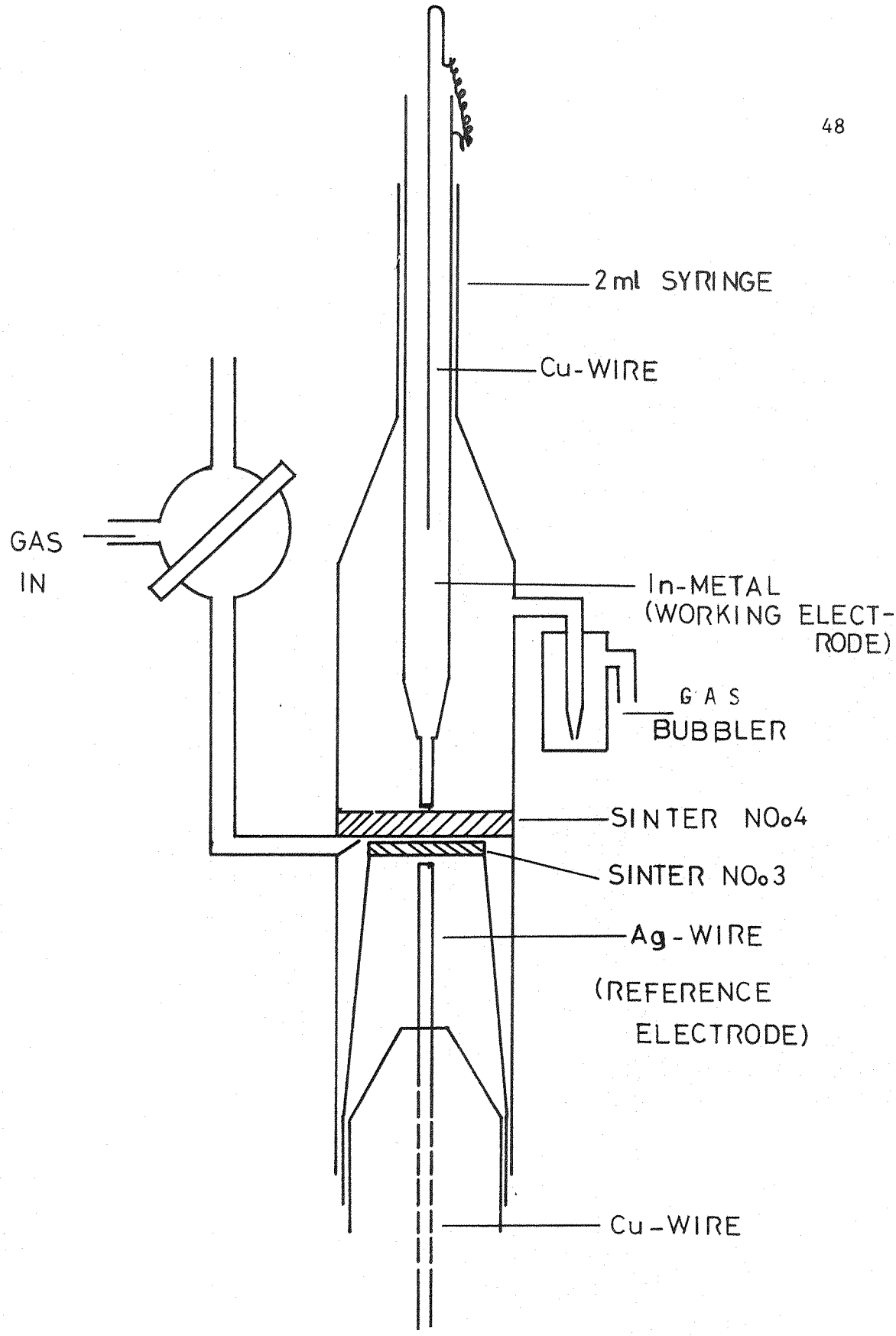

FIG. 3 SPECIAL DESIGN OF TWO COMPARTMENTS ELECTROLYTIC CELL

VII ELECTRODES

WORKING ELECTRODE (W.E.)

The working electrodes for cyclic voltammetry and other kinetic measurements was a platinum-wire about 0.05cm diameter and 1 cm long. The platinum electrodes were made by joining the desired platinum-wire to a length of the copper-wire and sealing part of the platinum into an extended cone glass joint of the required size.

The other working electrodes for cyclic voltammetry were made from indium (In-wire, supplied by Johnson Matthey Ltd;) as well as lead. The procedure for making the indium microelectrodes was as follows:- the indium wire was first melted inside a thick walled soft glass capillary of ∿ 0.05mm diameter; a section of the capillary containing the indium thread was then heated and drawn down until the required diameter was reached. This procedure could be repeated if necessary. Since indium can be made to wet glass it is possible to reach very small radii (down to 0.1μ) in this way. The diameters of the finest electrodes were determined from the kinetic measurements; that of the coarser electrodes was determined by microscopy.

Lead microelectrode were made by a somewhat different procedure: capillaries containing molten lead were drawn down on a glass blowing lathe but it found that a void appeared at the lead tip when the diameter was reduced to < 10μ presumably due to the much higher interfacial energy. The lead in the whole capillary was therefore melted and forced into the narrower parts by high pressure nitrogen.

VIII CLEANING OF CELLS

The cells were first cleaned with hot concentrated potassium hydroxide in alcohol, by filling the cell with the potassium hydroxide solution and allowing it to stand for about half an hour to remove grease. The cell was then washed with distilled water repeatedly by first allowing water to flow through and then filling with distilled water. The next stage was to clean the cell with chromic acid again followed by repeated washing with distilled water. Finally, the cell was washed with acetone and dried in an oven over night at 180°C.

A special method was used for the two compartment cell having the fine glass sinter disc. The cell was cleaned with acetone and then filled with acetone; nitrogen was bubbled through the cell for half an hour to remove all chemical precipitates from the sintered glass. The cell was then washed with water followed by chromic acid. It was then washed in boiling water for half an hour so as to remove chromic acid from sintered glass. Finally, it was dried in a vacuum oven over night at 150°C.

IX EXPERIMENTAL PROCEDURES

The solutions were prepared inside the dry-box which was filled with purified dry nitrogen. All the volumetric flasks were dried in the oven and cooled inside the dry-box, to prevent ingress of moisture.

For both slow sweeps and cyclic voltammetry results were taken from the first sweep of the potential scale, using a clean electrode. Cyclic voltammetry at various sweep speeds was used to investigate the reversibility of each of the hydrogen ion couples. Where comparisons of potentials were requires the observed potentials were measured against a silver/ silver ion electrode. In slow sweep experiments to determine half-wave potentials the aromatic hydrocarbon concentration was 10^{-3}M to 2.5×10^{-3}M and the slow sweeps range down to 5×10^{-4}V/s.

CHAPTER IV

CHAPTER IV

RESULTS AND DISCUSSION

Figure 6a,b,c, shows the experimental results for the first reduction step of a series of aromatic hydrocarbons, such as anthracene, 9-phenylanthracene, 9,10-diphenylanthracene, 9,10-dimethylanthracene, chrysene and perylene using cyclic voltammetry on conventional platinum wire electrodes. The experiments were usually carried out with substrate concentrations of 10^{-3}M, the supporting electrolytes were always tetraalkylammonium salts, (generally 10^{-1}M tetraethylammonium tetrafluoraborate Et_4NBF_4) and the reference electrode was silver/ silver ion with 10^{-2}M ($AgNO_3$) silver nitrate.

The characteristics of these plots such as the peak separation for the forward and reverse sweeps (fig.6a,b,c,) and the linear plots of the peak current (i_p) against the square root of the sweep rate ($\nu^{\frac{1}{2}}$) (figs.7a,b,c,) show the processes to be typically diffusion controlled, the electrode reaction being throughout in equilibrium. Furthermore these measurements show that the radical anions formed on the forward sweep are stable on the time scale used in the measurements since their reoxidation follows the predicted pattern. Clearly therefore there are no complicating features such as reactions with proton donors.

These results are consistent in every way with previous measurements by means of polarography and single and cyclic sweep voltammetry. The further reduction of the anion radicals to form reactive dianions fig.6a,b,c, is also in line with previous investigations.

For DPA these have shown that although the second charge transfer is chemically reversible in DMF in the presence of Bu_4N^+ ion it is decidedly electrochemically irreversible[61a]. When much lower concentrations of Et_4N^+ ion are used, the second charge transfer becomes reversible. Reversible reduction of perylene^{o-} to perylene^{--} has been observed in several common aprotic electrochemical solvents. The effect of the solvent upon the redox potentials of perylene has been determined and both charge transfer steps have been found to be reversible for the compound in DMF, acetonitrile etc. The experiments show that chrysene is very difficult to reduce, the peak potential for the first charge transfer being -2.25V in DMF. The experiments identify the species reacting with the dianion as being a solvent impurity, which is destroyed by the background current, rather than either the solvent or electrolyte.

The potential of the first reduction step of perylene in DMF has been shown to be morw or less independent of the supporting electrolyte cation, such as Et_4N^+, Bu_4N^+, and Me_4N^+ [62a]. On the other hand ΔE^o is ≃ 59.5mV in the presence of the largest ion and only 54.5mV in Et_4N^+ containing solution. For anthracene, the first charge transfer is nearly independent of the supporting electrolyte. A number of electrochemical investigations have dealt with weak ion-pairing effects and the effect of tetraalkylammonium ions on the reversibility of alkali metal ion reductions has been discussed. Reduction has been found to be irreversible in the presence of Me_4N^+ and Et_4N^+ ions and reversible in the presence of large ions. Peover[63a] makes the following statement: " In these solvents(those of low dielectric constant) solvation of

the tetraalkylammonium ions is apparently so weak that they are smaller and therefore interact more strongly with large diffuse anions than do alkali metal cations".

Overall the balance of evidence is that the first reduction steps at least are reasonably simple with only minor complications due to ion pairing and these reactions were therefore chosen for further investigation using the micro-electrodes.

The data for two separate indium microelectrodes at two different ranges of sweep speeds and using similar concentrations of perylene as substrate are illustrated in fig.8. It is noteworthy that voltammograms may be obtained using electrodes as small as $\sim 3\times10^{-10}cm^2$ and current scales down to 100pA full scale deflection. It may be seen that at the higher sweep speeds the pattern of behaviour is similar to that observed with the conventional platinum electrodes so that the cyclic voltammograms are dominated by the transient terms which have the same form as those predicted for planar diffusion fields, equation 2.13. At the lower sweep speeds (and to some extent over the whole range) the plots of i_p versus $\nu^{\frac{1}{2}}$ are curved fig.8e. The key data derived from figs 6 and 8 are given in Table 3 and 4. It is noteworthy that while $i_{p_a}/i_{p_c} \simeq 1$ at all sweep rates (in the higher ranges) the peak separation differs significantly from the expected 60mV for the indium microelectrodes. It is possible that these experimental curves might be affected by ohmic potential drops, impurities in the solvent, starting material or supporting electrolyte. An effect of impurities is unlikely in view of the extensive purification procedures adopted and the entirely normal behaviour of the cyclic voltammograms on conventional platinum wire electrodes. Delahay[54a] has derived a rough correction for the effects of ohmic losses on diffusion controlled reactions measured with rotating disc electrodes

and his corrected curve is shown in fig.9. It has been noted, however, that ohmic potential drops are unlikely to affect transients on electrodes of these dimensions. The deviations from the form of the voltammograms predicted for planar electrodes is therefore much likely to be due to the contribution of the steady state current caused by the superposition of a spherical diffusion field. It may be seen that at low sweep speeds, fig. 8b the plots do indeed approach the shape of a conventional steady state voltammetric curve as determined for example in stirred solution using rotating disc electrode or by polarography. The sweep speed at which this transition is observed depends on the size of the electrodes being higher the smaller the radius fig. 10. This is expected since the rate at which an equilibrium spherical diffusion field will be established will increase with decreasing electrode size. The further analysis of the voltammograms according to the theory for reversible processes (equation 2.2.18) or irreversible processes(equation 2.3.31) is therefore best carried out on data obtained at the lowest sweep speeds.

Substitution of the data for an electrode of approximate radius into equation (2.2.19)

$$i_D/i_D-i = k \exp-bt$$

gave plots of log i_D/i_D-i against potential (E), fig. 11. The set of straight lines has slopes between 53mV and 55mV, which are only slightly different from the theoretical valve 59.1mV. The experiments were carried out of using concentrations 1.0mM, 1.5mM, 2.0mM and 2.5mM in

the same concentration of supporting electrolyte.

It is evident that the voltammograms are close to those predicted for diffusion control of the reaction. The data at low and high overpotentials, fig. 11 (and particularly at low potentials) however deviate from the predicted line the currents apparently being larger than those expected for diffusion control. It is possible that these deviations are due to residual contributions of double layer charging currents in regions where the faradaic current only varies slowly with potential. The shape of the voltammograms for forward sweeps at low potentials however also suggested a contribution by the reduction of adsorbed species. We note also that all voltammograms gave well defined limiting diffusion currents from which the radii of the electrodes were estimated according to equation $i_D = FDC_o^{\infty}.2\pi r$ ie assuming a hemispherical tip.

The further analysis of the data for relatively large electrodes $r \simeq 5.9\mu$ according to the extended equation(2.3.31) which takes into account the effects of irreversibility of the electron transfer reaction is illustrated in fig.12 for the forward sweep of the voltammogram, fig.12. The standard potential used in the analysis was derived from the cyclic voltammograms measured at higher sweep rates. This value may differ from the true potential by virtue of differences in the diffusion coefficients and activity coefficients of the parent hydrocarbon and the derived radical anion. The analysis was therefore carried out both with the standard potential directly determined and values 20, 40, and 60mV more positive. The data derived to not correspond in any recongnisable way with equation (2.3.31). Firstly, the denominator vanishes

both at intermediate positive and negative values of the over-potential i the current lies above that for diffusion control as has already been noted; for E taken directly from cyclic voltammetry the denominator is in fact negative in the whole potential range. Secondly the Tafel slope is $\sim$ 60mV which is hardly consistent with irreversibility. Thirdly, the intercept for $E \sim E^{\theta}$ gives values of the standard rate constant $k_o \simeq 0.03 cms^{-1}$ which are low compared to published data for this type of system. Its evident that the rate of masss transfer to electrodes of these dimensions is not sufficiently high to permit the resolution of the rate of the electron transfer step; this is confirmed by the data as those in fig.11 which show that the reaction is in fact diffusion controlled in the region $E \simeq E^{\theta}$ for larger electrodes.

It is evident therefore that kinetic analysis using such quasi steady state data are only possible provided electrodes having a radius at least one order of magnitude smaller are used; optimal conditions will be for the reverse sweep at low sweep rates (10^{-4}V/s used here) since this will permit the maximum time for establishing steady state conditions and minimize the effects of adsorption at low potentials. Data for the microelectrode of radius 10^{-5}cm ar shown in fig.13 again using four values of the standard potential here spaced at 10mV intervals. It may be noted that the standard potentials as derived from cyclic voltammograms used in the various analysis differ, probably due to changes in potential of the silver/ silver ion electrodes. The plots derived are not, however particularly sensitive to the magnitude of the value of E^{θ} chosen.

The scatter in the derived data is large which is not surprising since the form of the denominator in equation (2.3.31) depends on the differences of comparable quantities, i being close to the diffusion

valve. It is of interest that the denominator again vanishes at low potentials if the value of E^{θ} derived directly from cyclic voltammetry is used; the range of applicability of the equation is extended as the chosen value of E^{θ} is made more positive. It is possible therefore that the conclusion that i lies above that for diffusion control is at least in part due to an incorrect choice of E^{θ} and this possibility should be confirmed by thermodynamic measurements.

The plots in fig. 13 nevertheless show that the data are in accord with a fast heterogeneous electron transfer reaction having a rate comparable to the rate of mass transfer. The Tafel Slope $\simeq$ 120mV is consistent with $\sim$ 0.5 while the intercept gives a standard rate constant constant $k_o \sim 1\ cms^{-1}$. This is comparable to the predicted rate of mass transfer $D/r \sim 1\ cms^{-1}$ and evidently equation (2.3.31) adequately corrects for the effects of diffusion. The rate constant derived is comparable to the values which have been measured by A.C. impedance methods and is probably also of comparable validity since k_o is high for evaluation by relaxation techniques. It appears from fig. 13 that rate constants up to 10 cms^{-1} may be fact be measurable by the steady state method developed here.

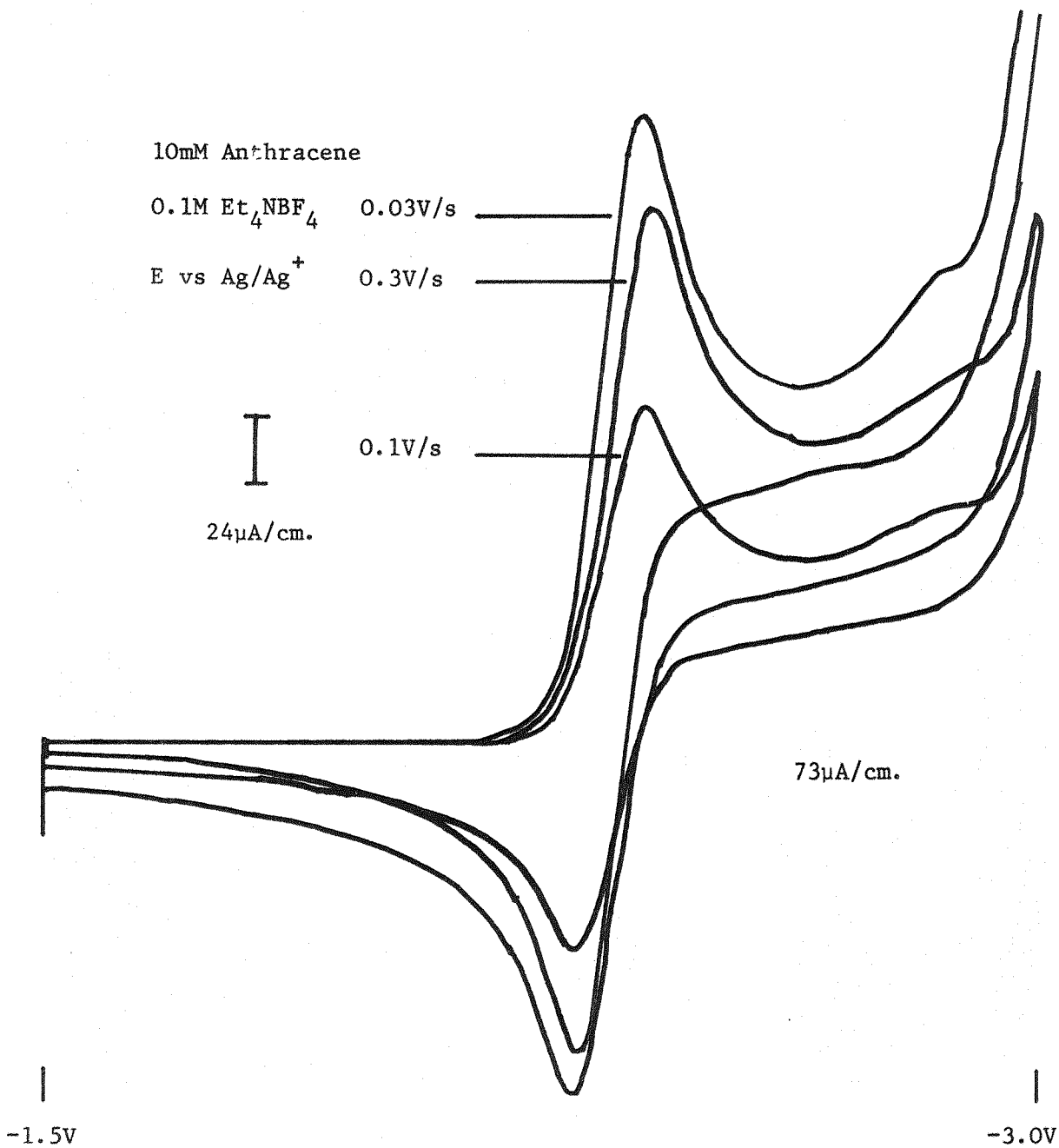

FIG. 6 a, Cyclic Voltammetry experiment for varying sweep rates on Anthracene.

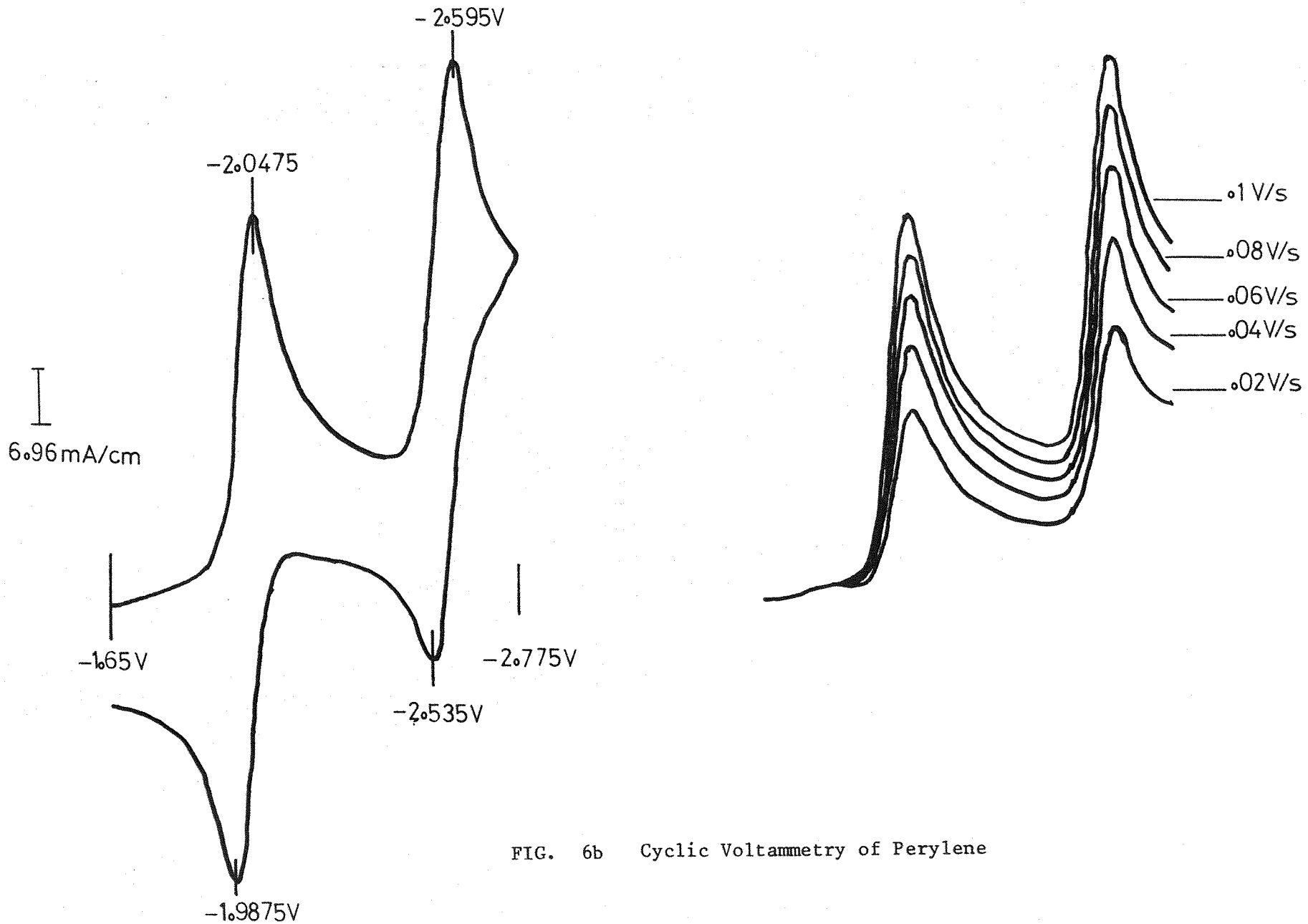

FIG. 6b Cyclic Voltammetry of Perylene

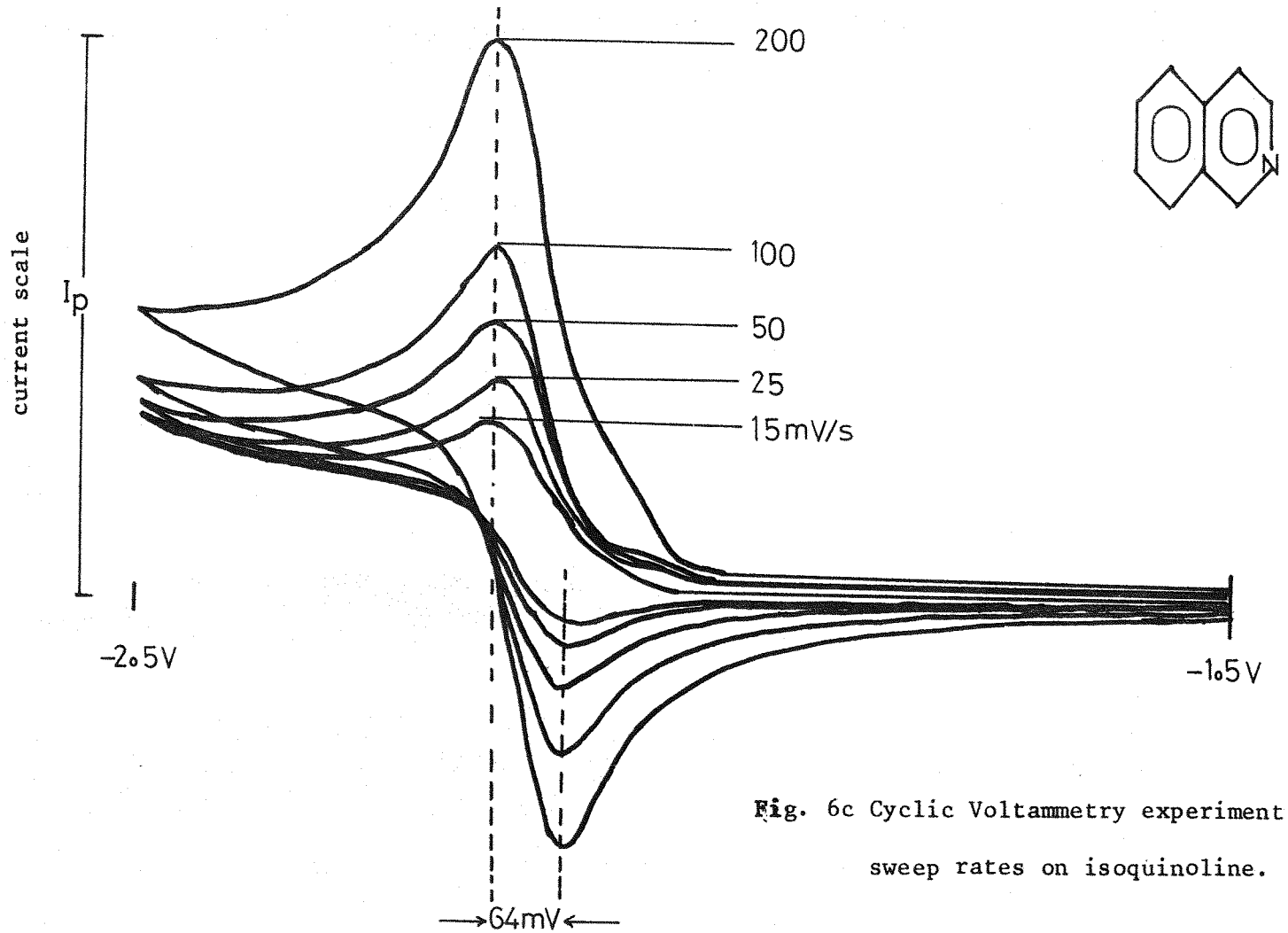

Fig. 6c Cyclic Voltammetry experiment for varying sweep rates on isoquinoline.

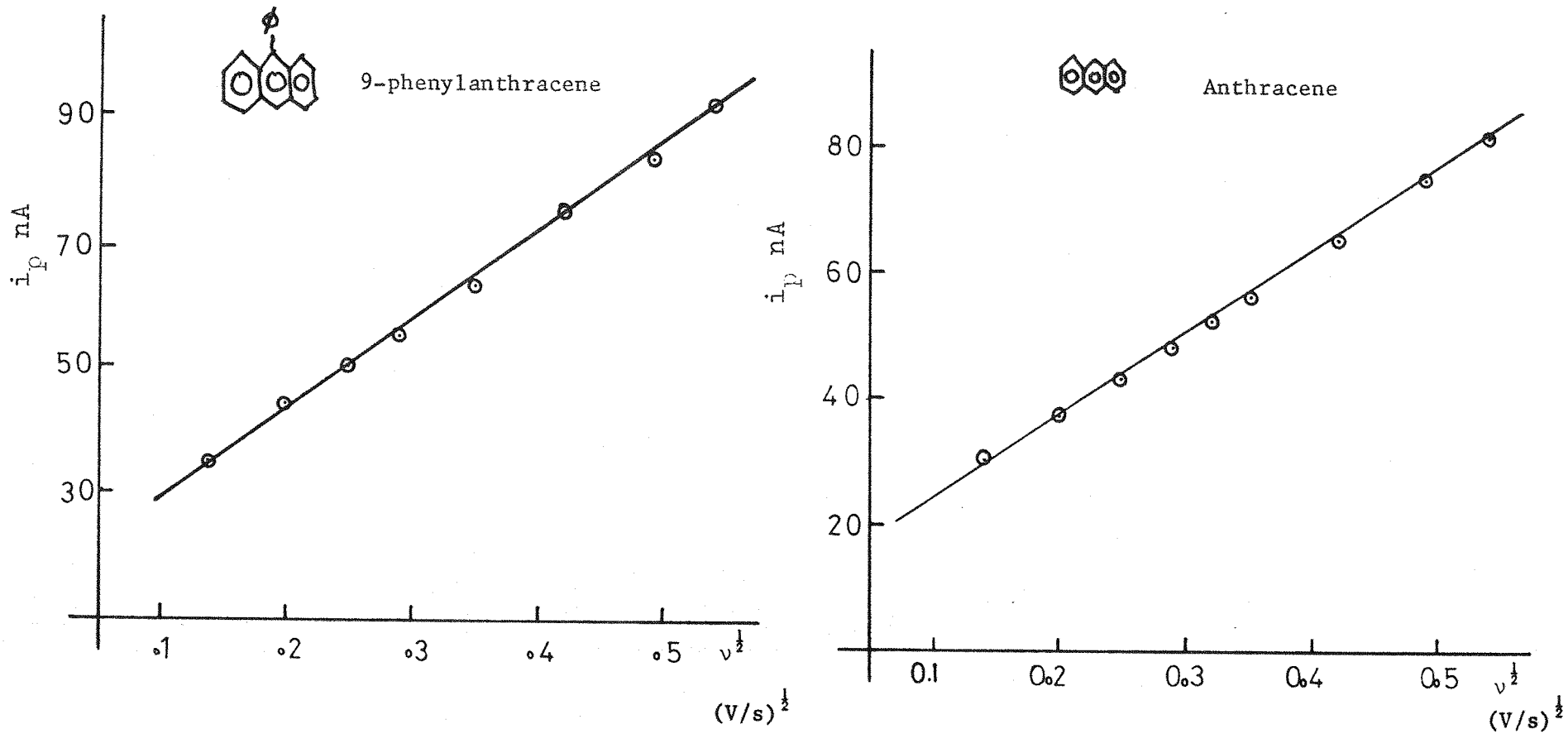
9-phenylanthracene
i_p nA
90
70
50
30
.1
.2
.3
.4
.5
$\nu^{\frac{1}{2}}$
$(V/s)^{\frac{1}{2}}$
Anthracene
i_p nA
80
60
40
20
0.1
0.2
0.3
0.4
0.5
$\nu^{\frac{1}{2}}$
$(V/s)^{\frac{1}{2}}$

FIG. 7a

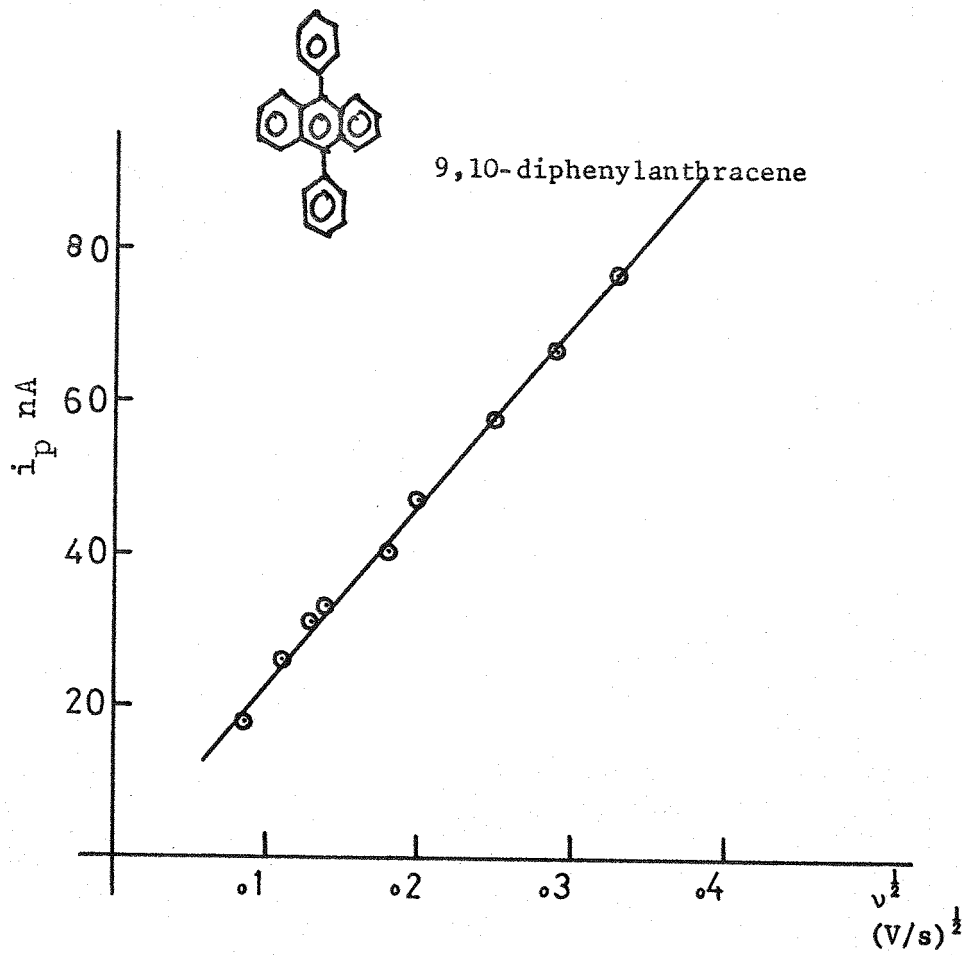
9,10-diphenylanthracene
80
60
40
20
i_p nA
.1
.2
.3
.4
$\nu^{\frac{1}{2}}$
$(V/s)^{\frac{1}{2}}$

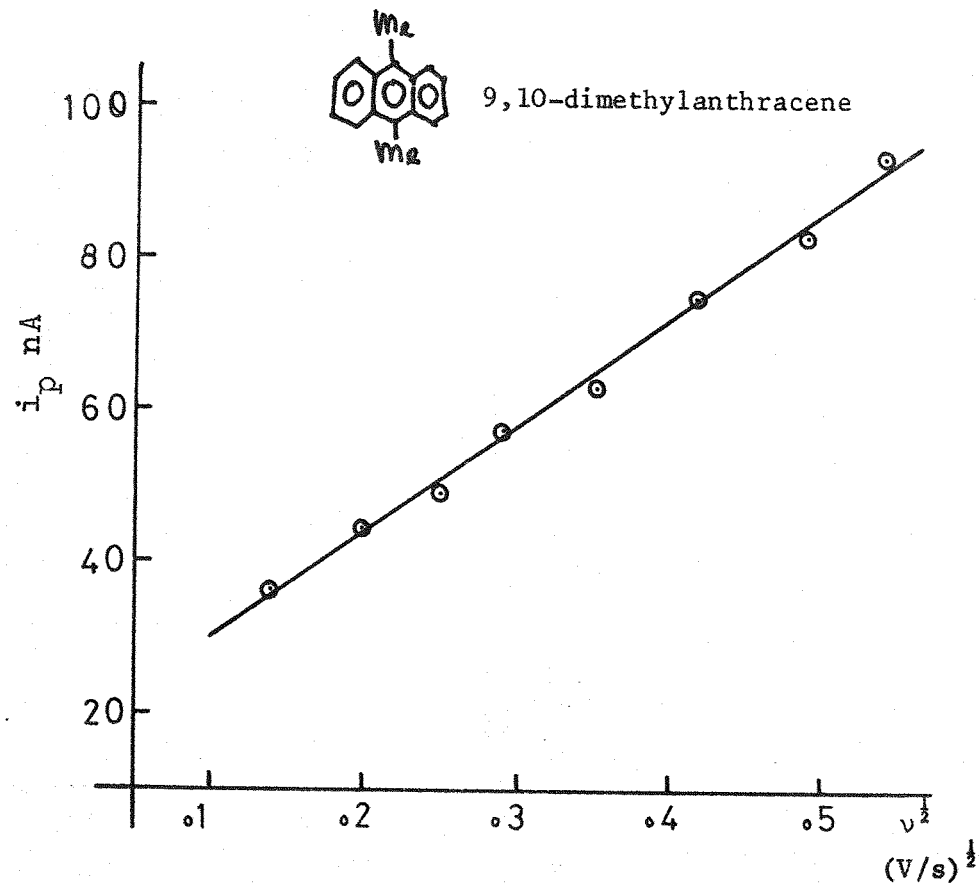
Me
Me
9,10-dimethylanthracene
100
80
60
40
20
i_p nA
.1
.2
.3
.4
.5
$\nu^{\frac{1}{2}}$
$(V/s)^{\frac{1}{2}}$

FIG. 7b

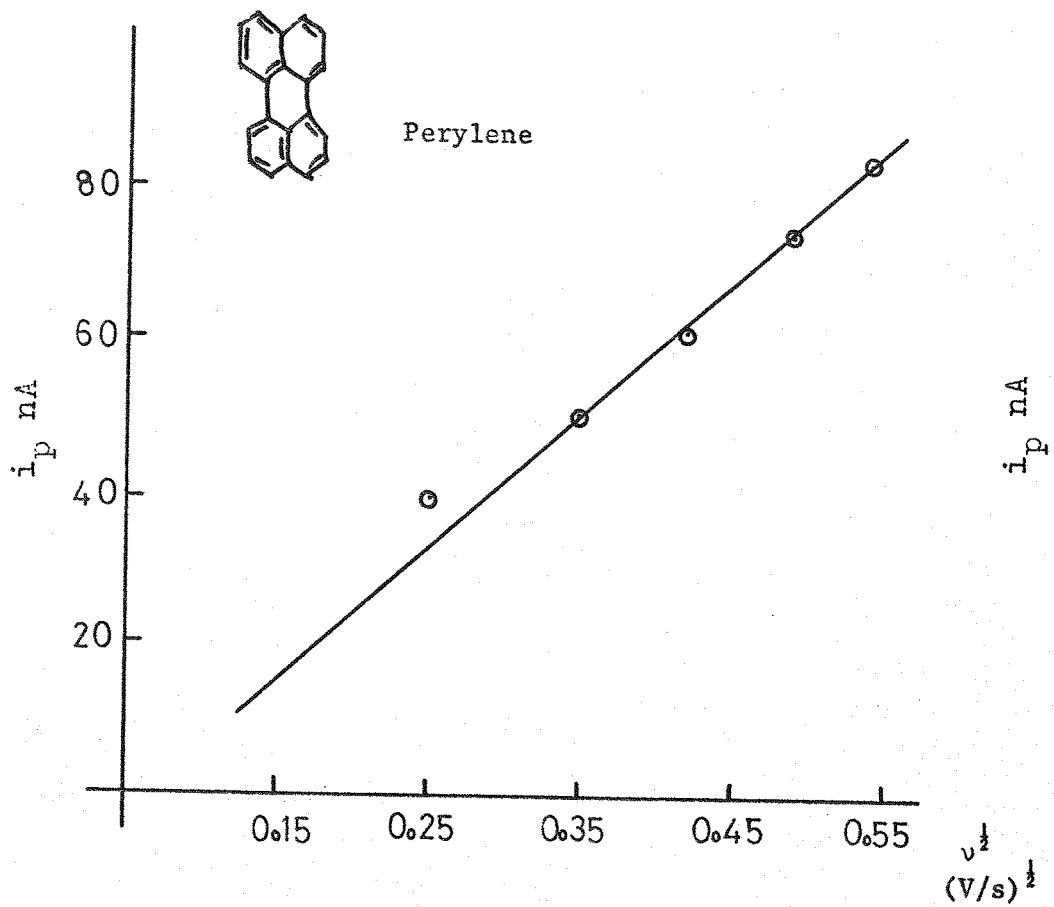
Perylene
80
60
40
20
i_p nA
0.15
0.25
0.35
0.45
0.55
$\nu^{\frac{1}{2}}$
$(V/s)^{\frac{1}{2}}$

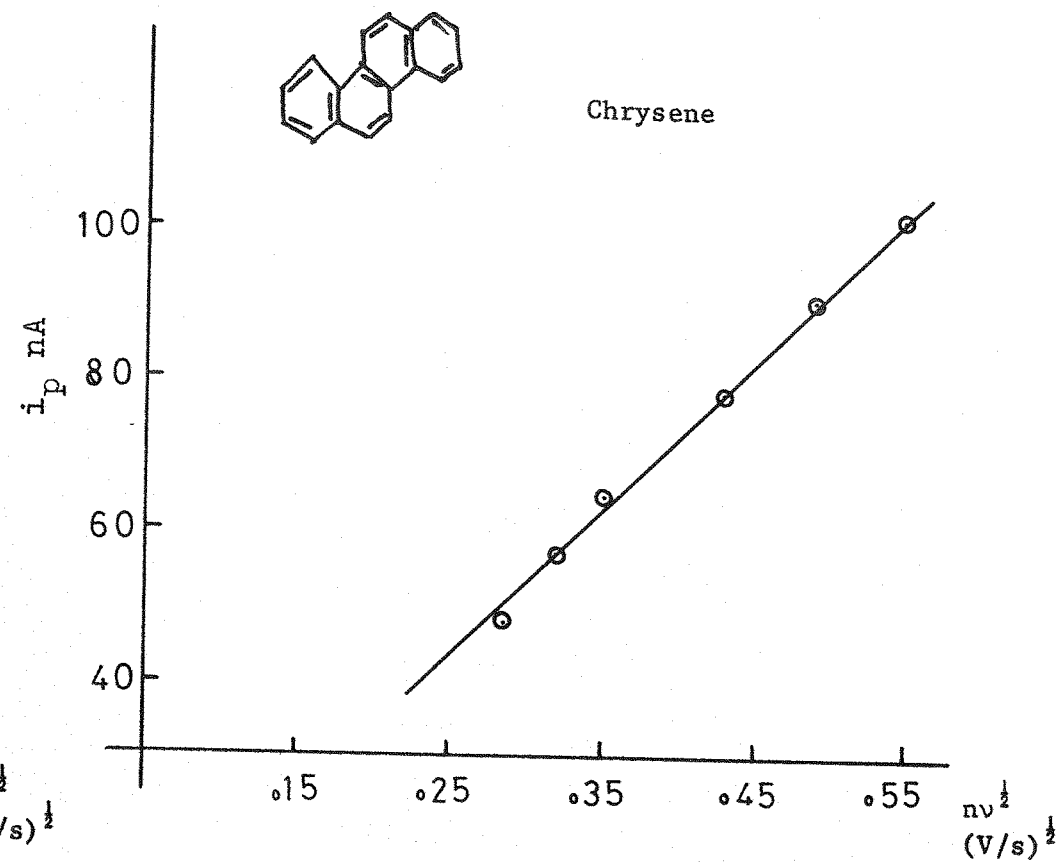
Chrysene
100
80
60
40
i_p nA
.15
.25
.35
.45
.55
$n\nu^{\frac{1}{2}}$
$(V/s)^{\frac{1}{2}}$

FIG. 7c

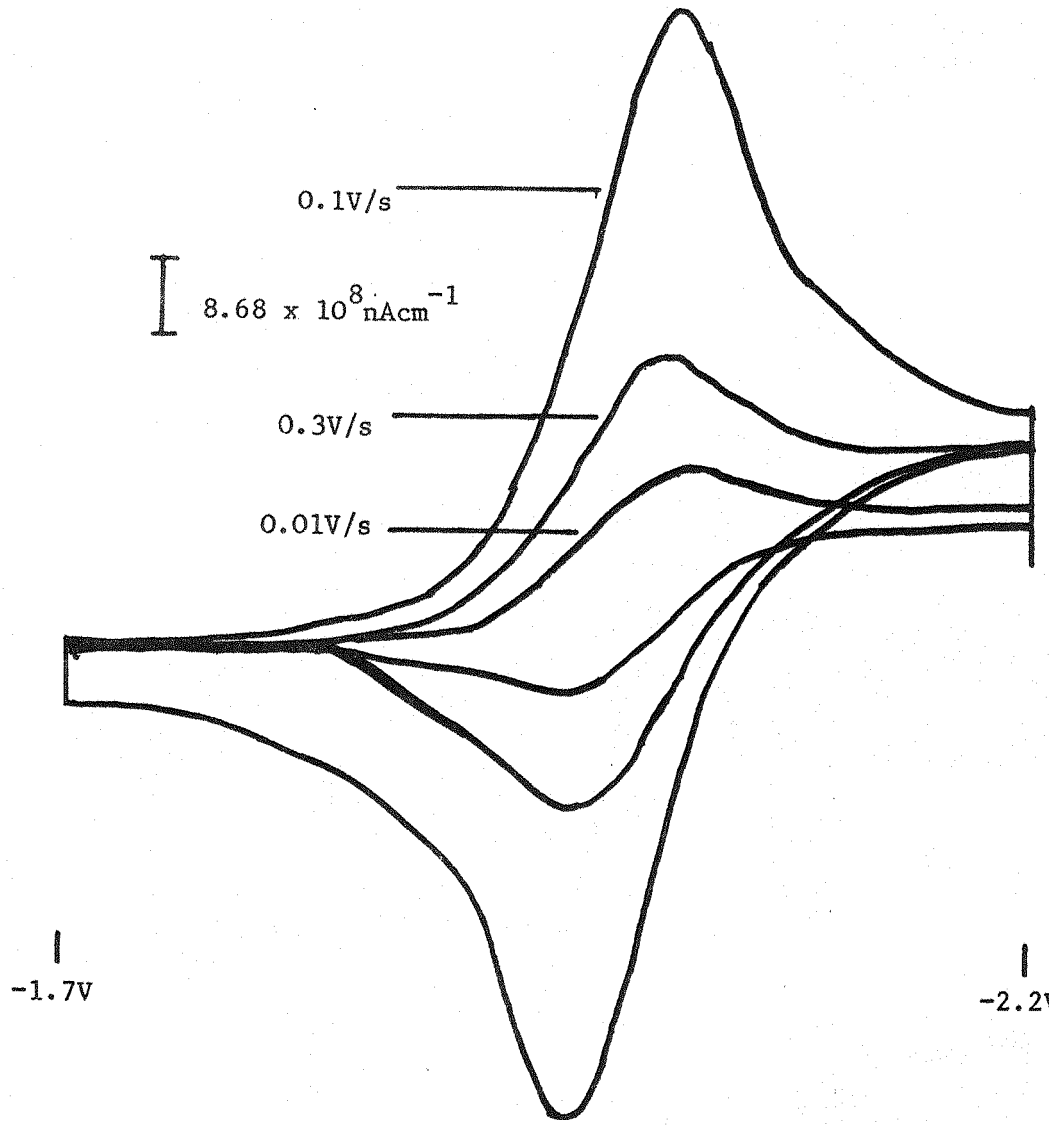

FIG. 8a. Cyclic Voltammetry experiment for varying sweep rates on Perylene with 0.1μ electrode.

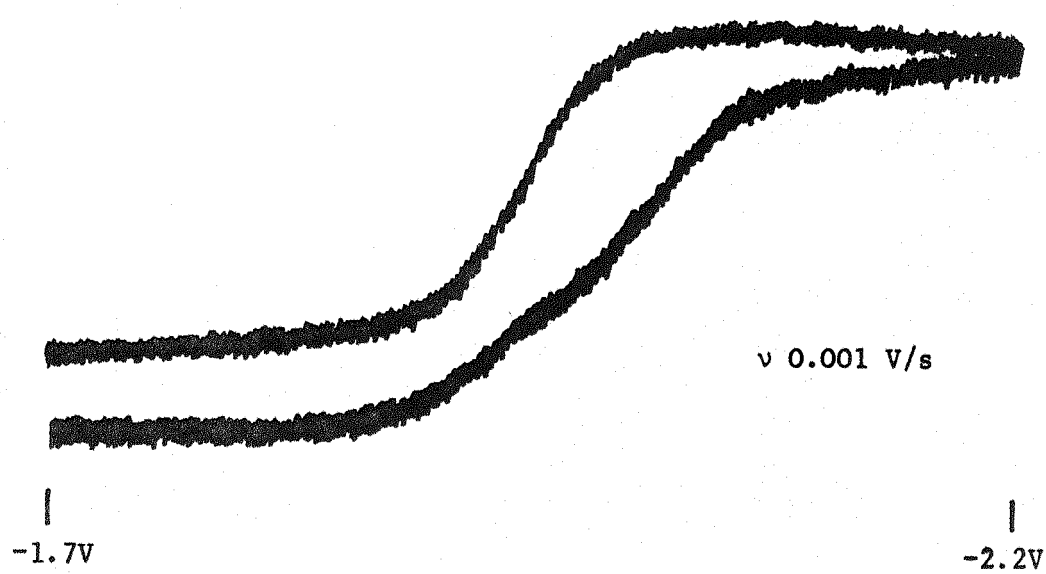

FIG. 8 b. Cyclic Voltammogram of Perylene in 1mM Et_4NBF_4/ 0.01M Ag/Ag^+ ion with 0.1μ In-electrode

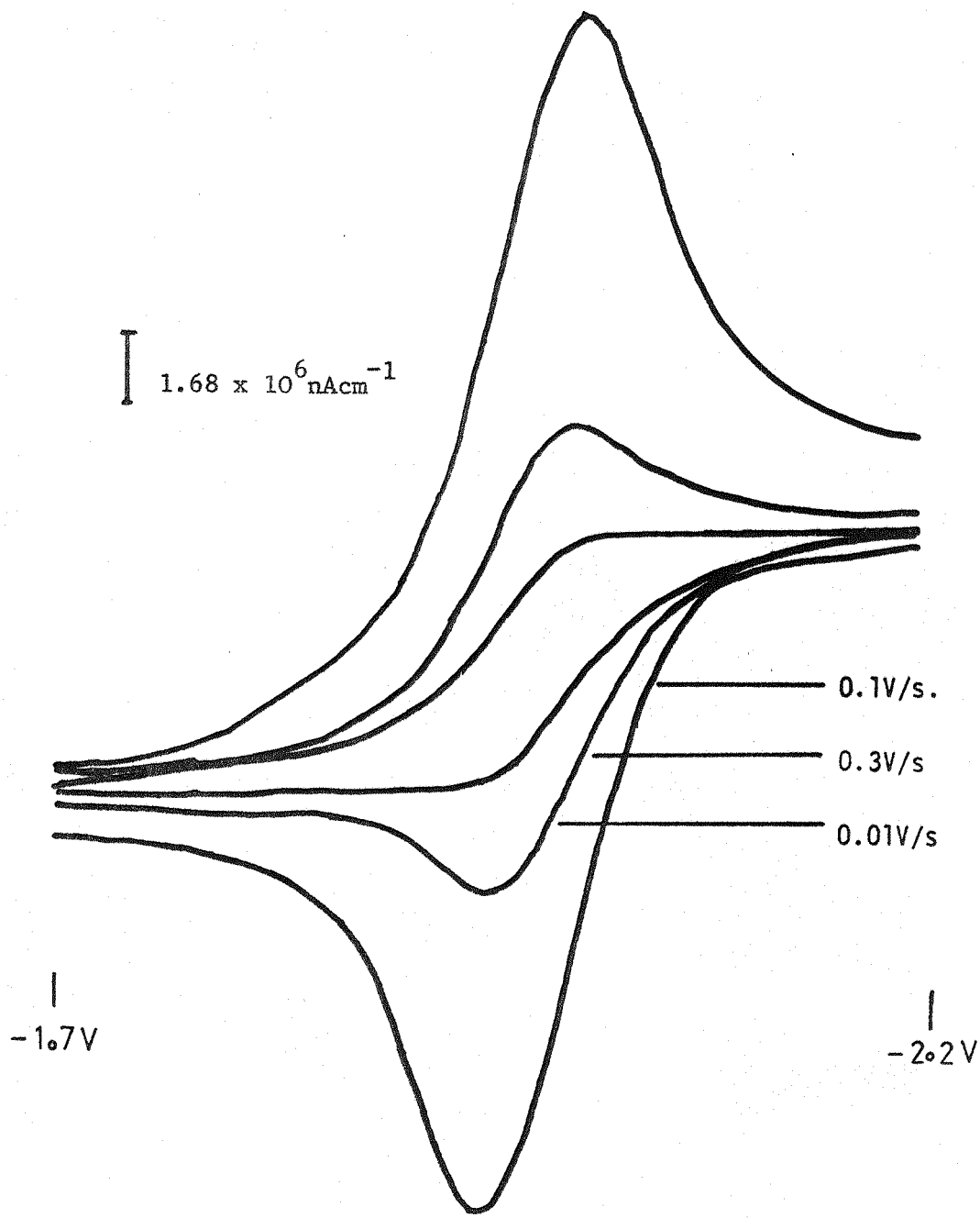

FIG. 8c. Cyclic Voltammetry experiment for varying sweep rates on Perylene with 5.9μ micro-electrode.

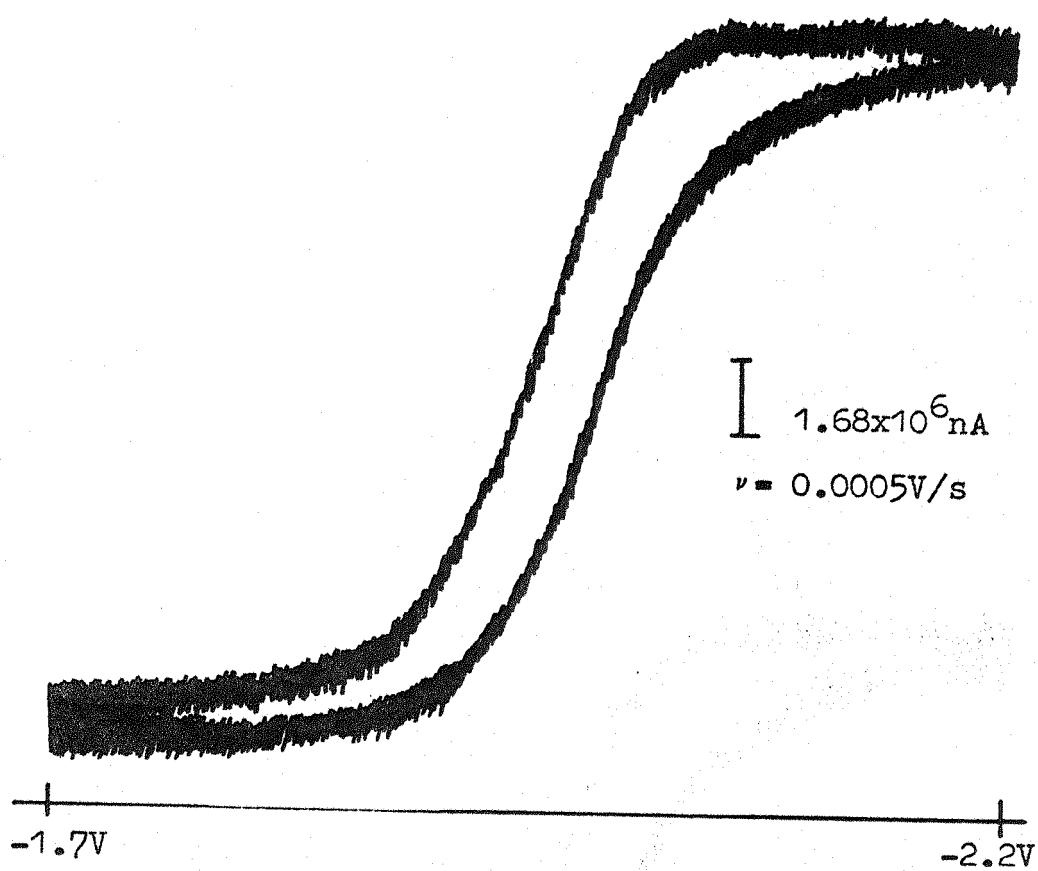

FIG. 8d. Cyclic Voltammogram of Perylene in 1mM/0.1M Et_4NBF_4/0.01M Ag/Ag^+ ion with 5.9μ In-Electrode.

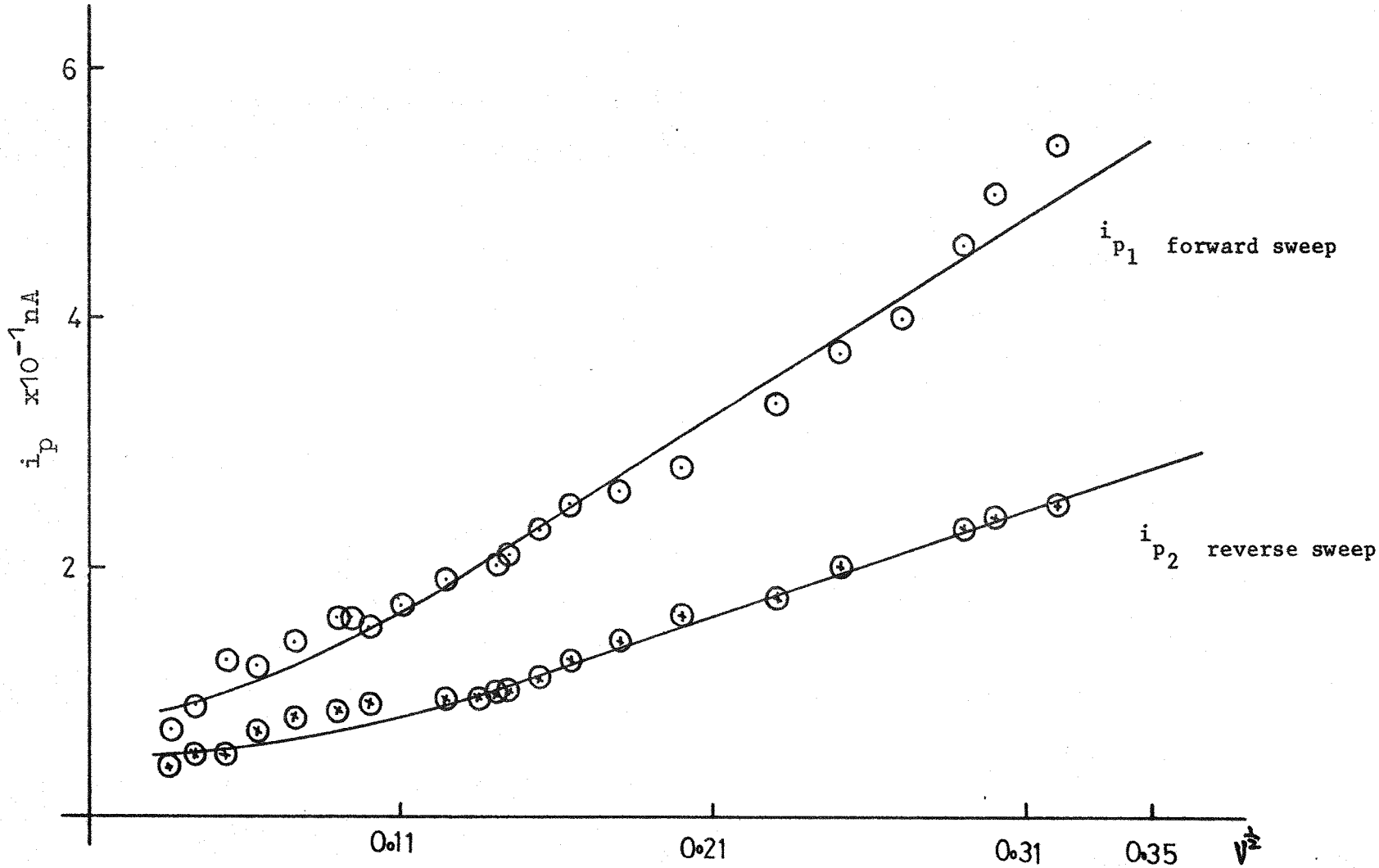

FIG. 8e Plots i_p vs $\nu^{\frac{1}{2}}$ of 10^{-3}M perylene/$10^{-1}Et_4NBF_4$/$10^{-2}Ag/Ag^+$ in DMF with In-electrode

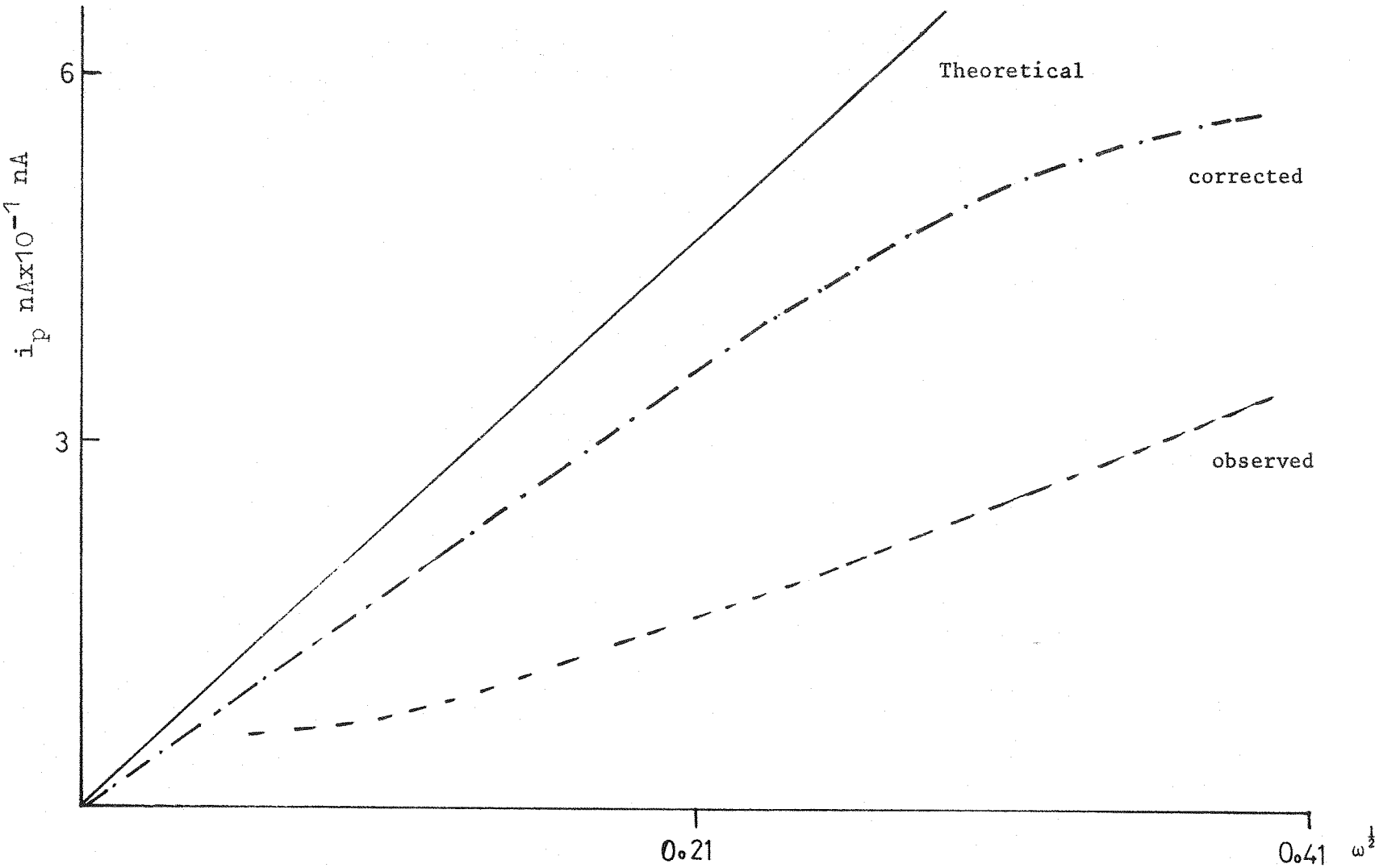
6
3
i_p nAx10^{-1} nA
Theoretical
corrected
observed
0.21
0.41
$\omega^{\frac{1}{2}}$

FIG. 9

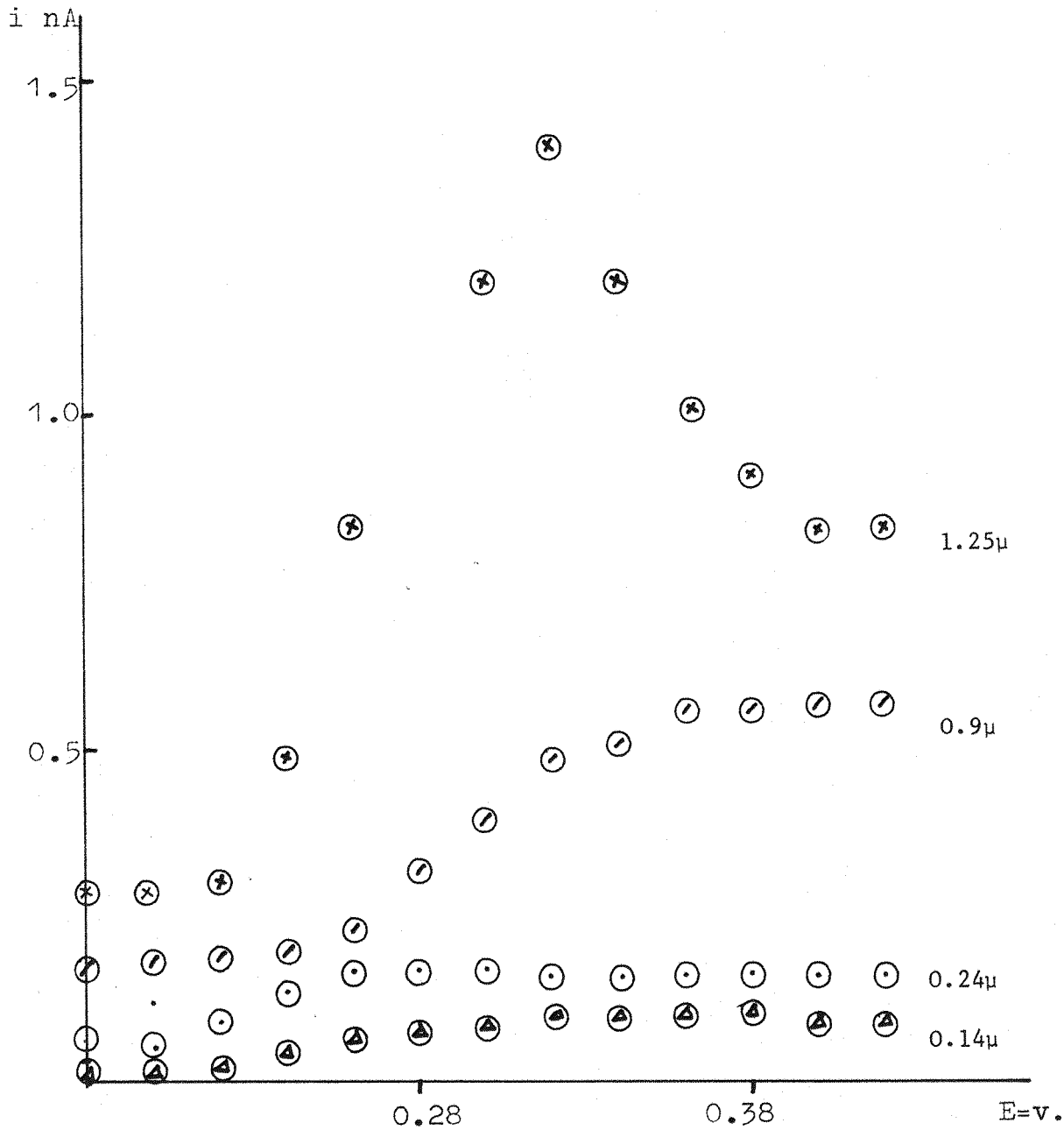

FIG. 10

Voltammetric data for the microelectrodes recorded at 0.001V/s.

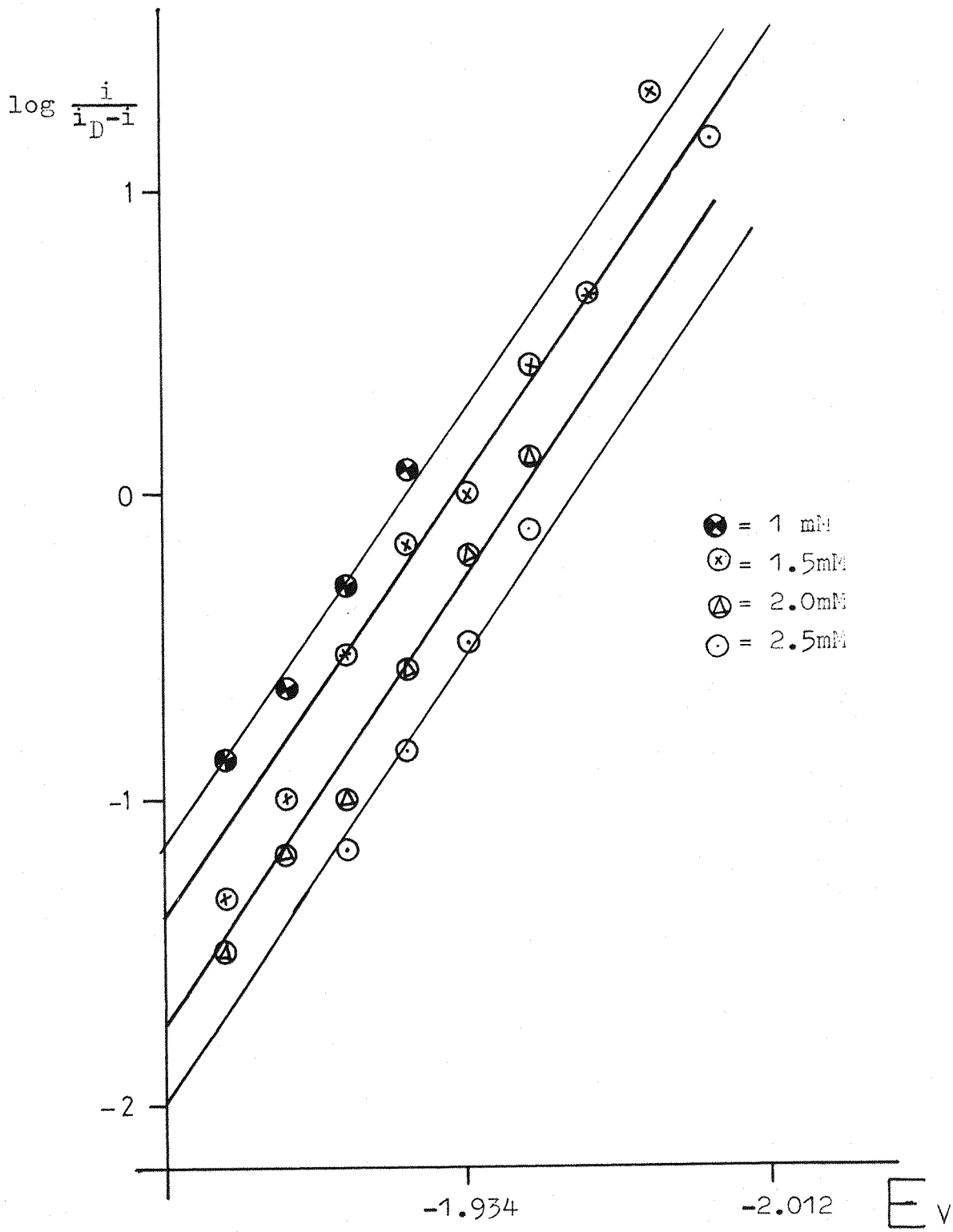

FIG. 11 plots $\log\frac{i}{i_D-i}$ vs E

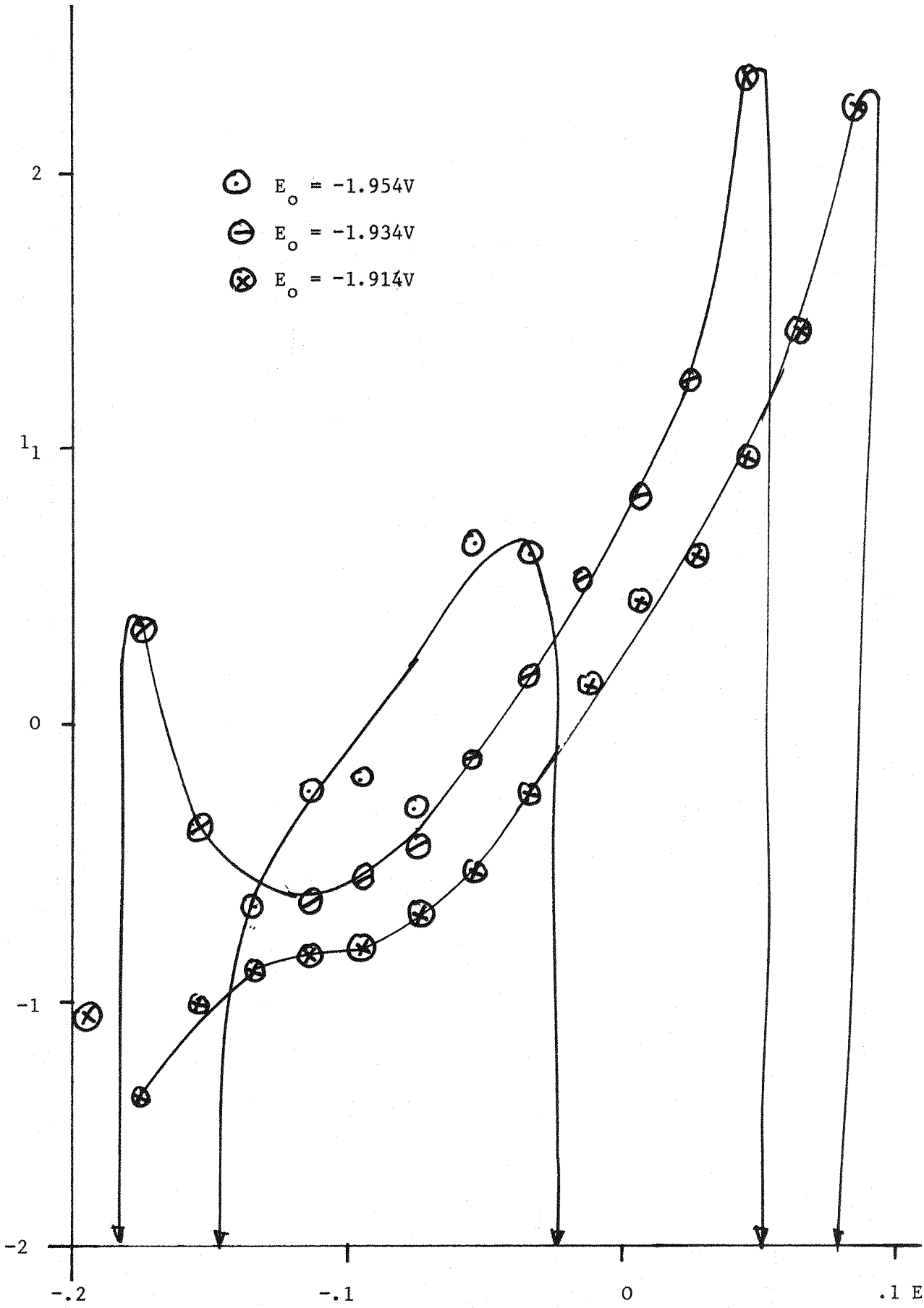

FIG. 12. Potential with respect of standard potential V.

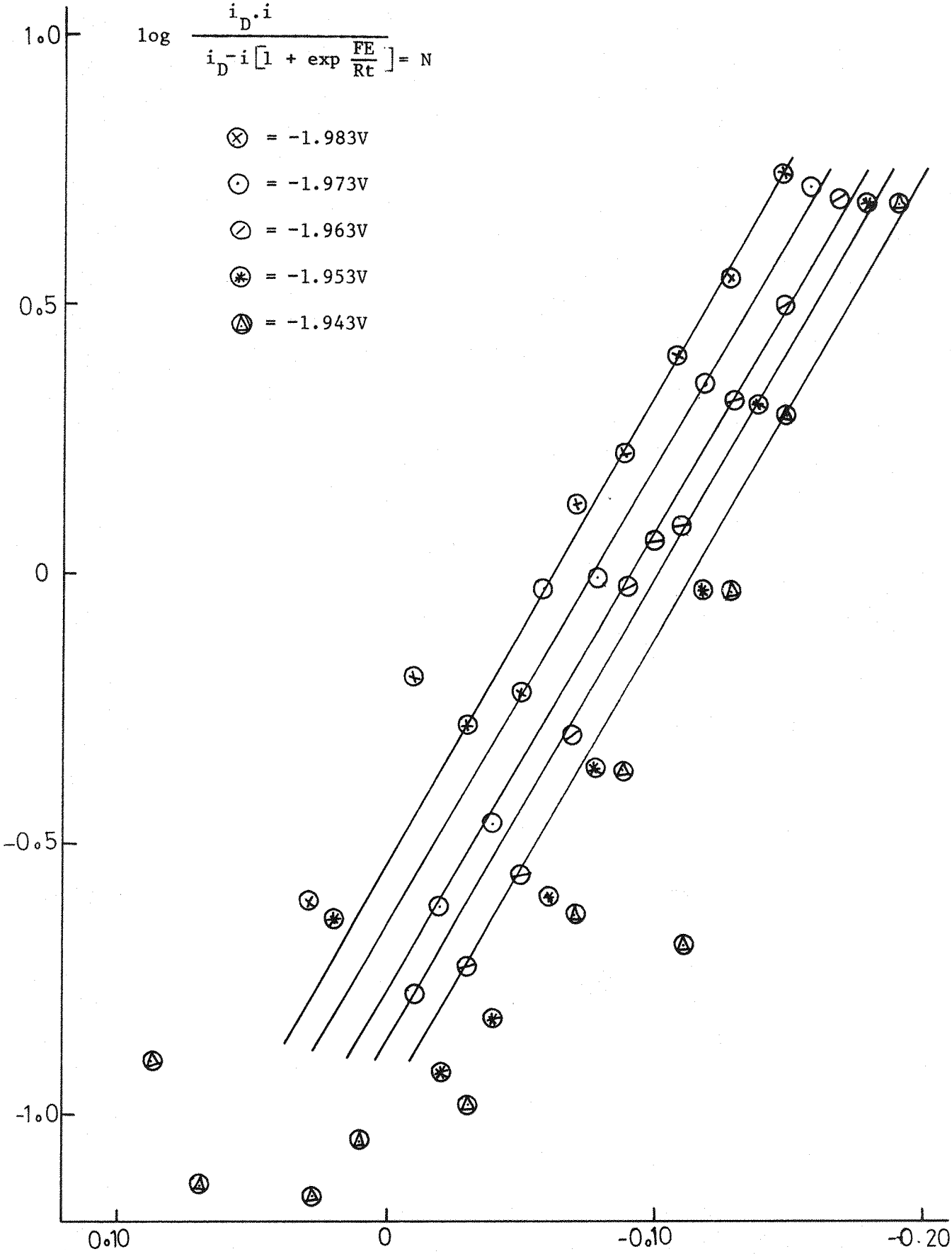

FIG. 13

Potential with respect of standard potential V.

TABLE 3

ν V/s	$\nu^{\frac{1}{2}}$ V/s	i_{p_1}	i_{p_2}	i_{p_3}	i_{p_4}	i_{p_5}	i_{p_6}
0.3	0.54	8.2	8.2	9.4	-	10.1	8.3
0.24	0.49	7.5	7.3	8.3	-	9.0	7.4
0.18	0.42	6.5	6.5	7.5	-	7.8	6.1
0.12	0.35	5.6	5.3	6.3	-	6.5	5.0
0.10	0.32	5.2	-	-	7.7	5.7	-
0.08	0.29	4.8	4.5	5.7	6.7	-	-
0.06	0.25	4.3	4.0	4.9	5.8	4.8	3.9
0.04	0.20	3.7	3.4	4.4	4.7	-	-
0.03	0.18	-	-	-	4.0	-	-
0.02	0.14	3.0	2.5	3.6	3.3	-	-
0.018	0.13	-	-	-	3.1	-	-
0.012	0.11	-	-	-	2.6	-	-
0.006	0.08	-	-	-	1.8	-	-

i_{p_1} = Anthracene

i_{p_2} = 9 Phenylanthracene

i_{p_3} = 9,10 dimethylanthracene

i_{p_4} = 9,10 diphenylanthracene

i_{p_5} = Chrysene

i_{p_6} = Perylene

Table of peak currents for Pt electrodes (fig.7)

TABLE 4

ν V/s	$\nu^{\frac{1}{2}}$ V/s	i_{p_1} nA	i_{p_2} nA
0.1	0.32	0.25	0.54
0.09	0.30	0.24	0.50
0.08	0.29	0.23	0.46
0.07	0.27	0.21	0.40
0.06	0.25	0.20	0.37
0.05	0.23	0.175	0.33
0.04	0.20	0.16	0.28
0.03	0.18	0.13	0.25
0.027	0.165	0.125	0.25
0.024	0.155	0.11	0.23
0.021	0.145	0.10	0.21
0.020	0.140	0.10	0.20
0.018	0.135	0.09	0.20
0.015	0.125	0.086	0.19
0.012	0.11	0.08	0.19
0.010	0.10	0.07	0.15
0.009	0.095	0.07	0.16
0.008	0.09	0.08	0.16
0.006	0.077	0.075	0.14
0.004	0.064	0.068	0.12
0.003	0.055	0.05	0.125
0.002	0.045	0.05	0.09
0.001	0.033	0.04	0.07

Table of peak currents for forward and reverse sweeps on In microelectrode radius 0.1μ (fig.9)

Table 5a

i nA	E	$E-E^{\ominus}$	$i_D.i$	M	N	log N
0	-1.817	0.166	0			
0.0021	-1.837	0.146	0.00022	-0.527	-0.0004	-3.9
0.0032	-1.856	-0.127	0.00033	-0.377	-0.00088	-3.05
0.0064	-1.876	0.107	0.0066	-0.327	-0.002	-2.69
0.0129	-1.895	0.088	0.0013	-0.297	-0.004	-2.39
0.0193	-1.915	0.068	0.00198	-0.203	-0.0098	-2.00
0.0289	-1.934	0.049	0.00297	-0.117	-0.025	-1.60
0.0364	-1.954	0.029	0.0037	-0.047	-0.079	-1.10
0.045	-1.973	0.010	0.0046	-0.0101	-0.046	-1.33
0.0557	-1.993	-0.010	0.0057	+0.0089	0.64	-0.19
0.0686	-2.013	-0.03	0.0070	0.0139	0.51	-0.29
0.0814	-2.032	-0.049	0.0084	0.0089	0.94	-0.027
0.090	-2.052	-0.069	0.0093	0.0069	1.35	0.13
0.0943	-2.072	-0.089	0.0097	0.0059	1.64	0.215
0.0975	-2.091	-0.108	0.010	0.0039	2.56	0.408
0.0996	-2.111	-0.128	0.0102	0.0029	3.52	0.55
0.1007	-2.130	-0.147	0.0104	0.0019	5.47	0.74
0.1018	-2.150	-0.167	0.0105			
0.1029	-2.169	-0.186	0.0106			

$$E^{\ominus} = -1.983$$

$$i_D - i\left[1 + \exp\frac{FE}{RT}\right] = M$$

$$\frac{i_D.i}{i_D - i\left[1 + \exp\frac{FE}{RT}\right]} = N$$

Tabular data for fig.13 for analysis of voltammograms according to equation (2.3.31) for 0.1μ In microelectrode. Standard potentials chosen as shown.

Table 5b

i nA	$E-E^{\ominus}$	$i_D.i$	M	N	log N
0	0.156	0			
0.0021	0.136	0.0021	-0.3321	0.000632	-3.19
0.0032	0.117	0.00032	-0.2121	0.001508	-2.82
0.0063	0.097	0.00064	-0.1841	0.003476	-2.45
0.0129	0.078	0.00132	-0.1821	0.00724	-2.14
0.0193	0.058	0.00198	-0.1011	0.019584	-1.70
0.0289	0.039	0.00297	-0.0551	0.054	-1.26
0.0364	0.019	0.00374	-0.0091	0.4109	-0.37
0.0450	0	0.00462	+0.0129	0.359	-0.45
0.0550	-0.02	-0.00565	+0.0239	0.2364	-0.62
0.068	-0.04	-0.00699	+0.02014	0.347	-0.46
0.081	-0.059	-0.00833	+0.0149	0.5590	+0.025
0.090	-0.079	-0.00926	+0.00884	1.05	+0.021
0.094	-0.097	-0.00967	+0.0078	1.224	+0.08
0.099	-0.138	-0.01018	+0.0039	2.6102	+0.42
0.1007	-0.157	-0.01036	+0.00199	5.18	+0.72
0.1013	-0.177	-0.01042	+0.0019	5.48	+1.07
0.1029	-0.196	-0.01058	+0.0009	11.75	+1.07

E = -1.973V

Table 5c

i nA	E	$E-E^{\circ}$	$i_D.i$	M	N	log N
0	-1.817	.146	0			
0.0021	-1.837	.126	0.00022	-0.177	-0.0011	-2.95
0.0032	-1.856	.107	0.00032	-0.093	-0.0034	-2.46
0.0064	-1.876	.087	0.00065	-0.094	-0.0069	-2.16
0.0129	-1.895	.068	0.00132	-0.082	-0.016	-1.79
0.0193	-1.915	.048	0.00198	-0.032	-0.0618	-1.20
0.0289	-1.934	.029	0.00297	-0.0121	-0.245	-0.61
0.0384	-1.954	.009	0.00374	+0.0156	+0.139	-0.62
0.0450	-1.973	-0.01	0.00463	+0.0279	+0.165	-0.78
0.0557	-1.993	-0.03	0.00573	+0.0309	+0.185	-0.73
0.0685	-2.013	-0.05	0.0070	+0.0259	+0.270	-0.56
0.0814	-2.032	-0.069	0.0083	+0.0169	+0.49	-0.30
0.09	-2.052	-0.089	0.0092	+0.0102	+0.90	-0.045
0.0943	-2.072	-0.109	0.0097	+0.0079	+1.22	0.086
0.0973	-2.091	-0.128	0.010	+0.0049	+2.04	0.309
0.0996	-2.111	-0.148	0.0102	+0.0031	+3.29	0.51
0.1007	-2.130	-0.167	0.0103	0.00206		0.70

$E^{\circ} = -1.963$

Table 5d

i nA	E	$E-E^{o}$	$i_D.i$	M	N	log N
0	-1.817	0.136	0		0	
0.0021	-1.837	0.116	0.00021	-0.0972	-0.0021	-2.67
0.0032	-1.856	0.097	0.00032	-0.0432	-0.0074	-2.13
0.0064	-1.876	0.077	0.00065	-0.0312	-0.02	-1.69
0.0129	-1.895	0.058	0.0013	-0.0342	-0.038	-1.42
0.019	-1.915	0.038	0.0019	-0.0002	-0.095	-0.97
0.0289	-1.934	0.019	0.0029	+0.0138	+0.2	-0.69
0.036	-1.954	-0.001	0.0037	+0.00328	+0.112	-0.95
0.045	-1.973	-0.02	0.0046	+0.0388	+0.118	-0.93
0.055	-1.993	-0.04	0.0056	+0.0368	+0.15	-0.82
0.0685	-2.013	-0.06	0.0070	+0.0279	+0.25	-0.60
0.081	-2.032	-0.079	0.0083	+0.0188	+0.44	-0.35
0.09	-2.052	-0.099	0.0092	+0.0110	+0.83	-0.08
0.094	-2.072	-0.119	0.0096	+0.0088	+1.09	-0.037
0.0975	-2.091	-0.138	0.010	+0.0049	+2.04	-0.309
0.099	-2.111	-0.158	0.0101	+0.0037	+2.72	-0.43
0.1007	-2.130	-0.177	0.0103	+0.021	+4.93	-0.69
0.1001	-2.150	-0.197	0.0104	+0.0018	+5.26	-0.76

E^{o} = - 1.953V

Table 5e

i nA	E	$E-E^{o}$	$i_D - i$	M	N	log N
0	-1.817	0.126	0			
0.0029	-1.837	0.106	0.00021	-0.0322	0.0065	-2.18
0.0032	-1.856	0.087	0.00032	+0.0028	0.114	-0.94
0.0064	-1.876	0.067	0.00065	+0.0088	0.073	-1.13
0.0129	-1.895	0.048	0.0013	+0.0058	0.224	-0.64
0.019	-1.915	0.028	0.0019	+0.0271	0.0703	-1.15
0.0289	-1.934	0.009	0.0029	+0.0418	0.069	-1.16
0.036	-1.954	0.011	0.0037	0.0438	0.0844	-1.07
0.045	-1.973	0.030	0.0046	0.0448	0.10267	-0.98
0.055	-1.993	0.050	0.0056	0.0408	0.1372	-0.86
0.0685	-2.013	0.070	0.0070	0.0298	0.2448	-0.62
0.081	-2.032	-0.089	0.0083	0.0188	0.419	-0.37
0.090	-2.052	-0.109	0.0092	0.0128	0.718	-0.14
0.094	-2.072	-0.129	0.0096	0.0088	1.090	-0.037
0.0975	-2.091	-0.148	0.0100	0.0051	1.960	+0.29
0.099	-2.111	-0.168	0.0101	0.0037	2.22	
0.1007	-2.130	-0.187	0.0103	0.0213	0.483	
0.101	-2.150	-0.207	0.01038	0.0021	1.9	
0.1029	-2.169	-0.236	0.0105	0.0018		

E =-1.943

TABLE 6

E	$\log\frac{i}{i_D-i}$ 1.0mM	$\log\frac{i}{i_D-i}$ 1.5mM	$\log\frac{i}{i_D-i}$ 2.0mM	$\log\frac{i}{i_D-i}$ 2.5mM
-1.8716	-0.870	-1.500	-1.180	-1.300
-1.8872	-0.630	-1.200	-0.850	-1.000
-1.9028	-0.300	-1.000	-0.480	-0.500
-1.9184	+0.080	-0.560	-0.075	-0.160
-1.9340	+0.700	-0.170	+0.340	0.000
-1.9496	-	+0.130	+0.640	+0.430
-1.9652	-	+0.670	+1.170	+0.650
-1.9808	-	+1.430	-	+1.320
-1.9964	-	+0.930	-	
-2.0120	-	+1.000	-	
-2.0270	-	-	-	

Analysis of cyclic voltammetric data for 1μ. In microelectrode at different concentrations of perylene according to equation (2.3.26) (Fig.11)

TABLE 7

E	0.14 μ	0.24 μ	0.9 μ	1.25 μ
0.18	.009	.027	.068	.130
0.20	.013	.050	.119	.160
0.22	.020	.090	.170	.300
0.24	.038	.130	.187	.500
0.26	.060	.156	.220	.830
0.28	.070	.160	.300	1.200
0.30	.080	.156	.390	1.400
0.32	.087	.148	.477	1.200
0.34	.090	.150	.510	1.000
0.36	.090	.150	.545	.900
0.38	.090	.150	.545	.800
0.40	.087	.150	.560	.780

Current-voltage data for different sized In microelectrodes in 1 mM solutions of perylene recorded at 0.0001 V/s (fig.10)

REFERENCES:-

1. M. Le Blanc - Z. physik. chem; 12 333 1893

2. E. Salomen - Z. physik. chem; 24 55 1897

3. J. Heyrovsky and M. Shikata - Rev. Trav. Chim. 44 496 1925

4. H.A. Laitinen and I.M.Kolthoff - J. Phys. Chem; 45 1079 1941

5. L.A. Matheson and N.Nicholson - Trans.Am.Electrochem.Soc; 73 193 1938

6. H.F. Weber - Wied Ann. - 7 536 1879

7. I.M.Kolthoff and J.J.Lingane - Polarography, Wiley, interscience, N.Y. 2e 1952

8. J.R. Alden, J.Q. Chambers and R.N.Adams - J. electroanal. chem. 5 152 1962

9. H. Matsuda and Y. Ayabe - Z. Elektrochem; 59 494 1955

10. J.E.B. Randles - Trans. Faradays Soc; 44 327 1948

11. A Sevcik - Collection Czecho. Chem. Commun. 13 349 1948

12. P.Delahay - J. Am. Chem. Soc; 75 119¼ 1953

13. W.H. Reimuth - ibid. 79 6358 1957

14. T.Berzins and P. Delahay - ibid. 75 555 1953

15. R.S.Nicholson and I.Shain - Anal. Chem. 36 706 1964

16. W.H.Reimuth - ibid. 33 185 1961

17. R.S.Nicholson - J. Am. Chem. Soc; 76 2539 1954

18. G.J.Hoijtink - Ric. Sci. Suppl; 30 217 1960

- Rec. Trav. Chim; 76 885 1957

M.E.Peover - Electroanalytical Chemistry, A.J.Bard, Ed; Marcel Dekker Inc.,N.Y. Vol.2.

19. S.Wawzonek and H.A.Liaitien - J. Am.Chem. Soc; 64 1765, 2365 1942

20. S.Wawzonek and J.Wang Fan - J. Am. Chem. Soc; 68 2541 1946

21. G.H.Hoijtink, J.Van Schooteen etc - Rec. Trav. Chim. 73 355 1954

22. P.H.Given - J. Chem. Soc; 2684 1958

23. A.Streitwieser and I.Schwager - J. Phys. Chem; 66 2316 1962

24. R.Pointeau - Ann. Chem. 7 669 1962

25. S.Wawzonek, R.Berkey and E.W.Blaha etc - J. Electrochem. Soc; 102 235 1955

26. A.C.Allison, T.A.Gough and M.E.Peover - Nautre 197 764 1963

27. D.E.G.Austen, D.E.J.Ingram, P.H.Given and M.E.Peover - Nature 182 1782 1958

28. R.Pointeau, J.Favede and P.Delhaes - J. Chim. Phy; 61 1129 1964

28a. K.S.V.Santhanam and A.J.Bard - J. Am. Chem. Soc; 88 2669 1966

29. A.C.Aten, C.Buthker and G.J.Hoijtink - Trans. Faraday Soc; 55 324 1959

30. A.C.Aten and G.J.Hoijtink - Z. Physik. Chem.(Frankfurt) 21 192 1959

31. T.J.Katz, W.H.Reinmuth and D.M.Simth - J. Am. Chem. Soc; 84 802 1962

32. T.A.Gough, M.E.Peover - Polarography 1964 McMilliam, Lon. p1017

33. A.C.Aten and G.J.Hoijtink - Ad. in Polarography, Pergamon, OXFORD, 1961 777

34. D.L.Maricle - Anal. Chem. 35 683 1963

35. R.Dietz and M.E.Peover - Disc.Faraday Soc; 45 154 1968

36. R.D.Allendeserfer, P.H.Rieger - J. Am. Chem. Soc; 87 2336 1965

37. G.H.Aylward, J.L.Garnett and J.H.Sharp - Analyt. Chem. 39 457 1967

38. B.Philipp et al. - Chem. Abstracts 60 1878g

39. K.I.Tury'an et al - Chem. Abstracts 59 29b

40. R.E.Moskalyk et al - J. Pharm. Sci; 50 179 1961

41. F.Oehme - Chem. Abstracts 52 8419f

42. V.Z.Deal et al - Anal. Chem; 27 47 1955

43. A.B.Thomas et al - J.Am. Chem. Soc., 79 1848 1957

44. J.Allen et al - J.Pharm.Pharmacol; 9 990 1957

45. E.Bunel et al - J. Chem. Soc., 164 1970

46. J.N.Butler - Ad. Electrochem. and Electrochemical Engineering, P.Delahay and C.W.Tobias ed., Vol. 7 1970 p.151-175

47. H.E.Zuagg et al - Anal. Chem; 36 2121 1964

48. C.D.Ritchie et al - J. Am. Chem. Soc; 89 1447 1967

49. M.P.Susarev - Zhur. Priklad. Khim; 34 412 1961

50. T.M.Ivanova et al - Russ. J. Phys. Chem; 35 598 1961

51. Handbook of Chemistry and Physics The Chemical rubber Company, Cleveland, Ohio 50ed. 1970 p.B109

52. B.Kratochvil - Crit. Revs. Anal Chem; 1 (4) 415 1971

53. B.D.H. Chemical Company Ltd.

54a. A.Sevcik - Collection Czechoslov. Chem. Communs. 13 349 1948

55a. J.E.B.Randles - Trans. Faraday Soc., 44 327 1948

56a. P.Delahay - J.Am.Chem.Coc., 75 1190 1953

57a. H.J.S.Sand - Phil.Mag., 1 45 1901

58a. Z.Karoglanoff - Z. Electrochem., 12 5 1906

59a. P.Delahay - Anal. Chem., 27 478 1955

60a. A.P.Brown,P.Bindra,M.Fleischmann and D.Pletcher - J.Electroanal. Chem. 58 31-39 1975

61a. Bo.S.Jenssn and V.D.Parker - J.Am.Chem.Soc., 97:18 1975

62a. ibid.

63a. M.E.Peover - Electroanalytical Chemistry Vol.2 . A.J.Bard Ed; Marcel Dekker, N.Y. 1967 p. 19.

64a. P.Delahay and G.L.Stiehl - J.Phys. and Colloid Chem., 55 570 1951.

CHAPTER V

CHAPTER V

Novel Syntheses involving the Brown-Walker Reaction

This Chapter contains a brief summary of experiments carried out in the first year which were aimed at extending the synthetic applications of the Brown-Walker reaction using pulse electrolysis.

INTRODUCTION

The first experiments on the electrolysis of organic compounds were carried out by Faraday[1] who noticed the formation of gaseous organic products during the electrolysis of acetate solutions. The reaction was reexamined by Kolbe who developed the well-known Kolbe electrosynthesis of alkanes from carboxylic acids.

$$2RCOO^- \longrightarrow R_2 + 2CO_2 + 2e \qquad 5.1.1.$$

The scope of the reaction was further extended by Crum Brown-Walker

$$EtOOCRCOO^- \longrightarrow EtOOCR\text{-}RCOOEt + 2CO_2 + 2e \qquad 5.1.2.$$

to provide a route for long chain dibasic acids by the dimerization of shorter chain dibasic species. There has been considerable debate as to whether reactions of this type involve adsorbed or solution free intermediates. The former seems the most likely since reaction is very sensitive to electrode material; in aqueous solution it is necessary to use platinum electrodes at high anodic potentials.

Recently it has been established that different products are obtained on carbon[2-4]

$$\mathrm{RCOOH} \longrightarrow \mathrm{RCOO}^{\circ} + \mathrm{H}^{+} + \mathrm{e}^{-} \longrightarrow \mathrm{CO}_2 + \mathrm{R}^{\circ} \begin{cases} \nearrow \mathrm{R\text{-}R} \text{ (at Pt-electrode)} \\ \searrow \mathrm{R}^{+} + \mathrm{e}^{-} \end{cases} \qquad 5.1.3.$$

$$\mathrm{R}^{+} \xrightarrow{\text{(at carbon electrode)}} \text{products}$$

II KINETIC DESCRIPTION OF THE KOLBE REACTION

The possible reaction steps in the Kolbe synthesis may be formulated as follows

$$RCOO^- + M \underset{k_1'}{\overset{k_1}{\rightleftharpoons}} RCOO^o(M) + e^- \qquad 5.2.1.$$

$$RCOO^o(M) \xrightarrow{k_2} R^o(M) + CO_2 \qquad 5.2.2.$$

$$R^o(M) + R^o(M) \xrightarrow{k_3} R\text{-}R \qquad 5.2.3.$$

$$R^o(M) + RCOO^- \xrightarrow{k_4} R\text{-}R + CO_2 + e^- \qquad 5.2.4.$$

$$RCOO^o(M) + RCOO^- \xrightarrow{k_5} R\text{-}R + 2CO_2 + e^- \qquad 5.2.5.$$

Assuming adsorption under Langmuir[5] conditions the rate of these steps may be written as

$$V_1 = k_1 (1-\theta) C_{RCOO^-} \exp \frac{\alpha F \eta}{RT} \qquad 5.2.6.$$

$$V_1' = k_1 \theta \exp \frac{-(1-\alpha)nF}{RT} \qquad 5.2.7.$$

$$V_2 = k_2 \theta \qquad 5.2.8.$$

$$V_3 = k_3 \theta^2 \qquad 5.2.9.$$

$$V_4 = k_4 \theta C_{RCOO^-} \exp \frac{\alpha F \eta}{RT} \qquad 5.2.10.$$

Using the steady state approximation one obtains the coverage for the reaction route 5.2.1, 5.2.2, 5.2.4.

$$\theta = \frac{k_1}{k_1 + k_1' + k_4} \qquad 5.2.11.$$

and assuming, for example, that the ion discharge radical reaction is slow

$$k_4 \ll k_1' \ll k_1 \qquad 5.2.12.$$

one obtains

$$V_4 = \frac{k_4 k_1}{k_1'} C^2_{RCOO^-} \exp \frac{3F\eta}{2RT} \qquad 5.2.13.$$

It may be seen that the steady state is determined by the rate constant of the slowest step which may be multiplied by an equilibrium constant for any preceding fast step.

The Kolbe reaction has also been investigated in the non-steady state using repetitive square pulse electrolysis.[5~9] In this case it is necessary to solve the equation for the non-steady atate coverage of the surface of the electrode. For example, for the reaction sequence

$$A \underset{k_1'}{\overset{k_1}{\rightleftharpoons}} B \xrightarrow{k_2} C \qquad 5.2.14.$$

where B is present only in the adsorbed state while neither A nor C are adorbed the processes are linked through the coverage θ. The equation for the time dependent coverage is

$$\Omega \frac{d\theta}{dt} = k_1 C_A (1-\theta) - k_1'\theta - k_2\theta \qquad 5.2.15.$$

where Ω is the saturation coverage for the monolayer of surface (moles cm^{-2}). Any or all of the rate constants may be potential dependent.

Assuming for the non-steady state that at the beginning of each pulse θ = 0, the variation of coverage with time is given by

$$\theta = \frac{k_1 C_A}{k_1 C_A + k_1' + k_2} \{ 1 - \exp \frac{-(k_1 C_A + k_1' + k_2)}{\Omega} t \} \qquad 5.2.16.$$

and the rate of formation of the product by

$$\frac{dx}{dt} = \frac{k_1 C_A k_2}{k_1 C_A + k_1' + k_2} \left\{ 1 - \exp \frac{-(k_1 C_A + k_1' + k_2)}{\Omega} t \right\} \qquad 5.2.17.$$

The rate therefore approaches the expected steady state value

$$R_s = \frac{k_1 C_A k_2}{k_1 C_A + k_1' + k_2} \qquad 5.2.18.$$

with a characteristic time

$$\frac{1}{\delta} = (k_1 C_A + k_1' + k_2)\Omega \qquad 5.2.19.$$

which in contrast to the steady state is determined by the sum of the rate constants, that is by the fastest step of the reaction sequence. The method has been used to investigate both the Kolbe reaction and the related Hofer-Moest formation of alcohols.[10]

Pulse electrolysis has also been used to investigate the intermediates in the Brown-Walker oxidation of monoethyl malonate in aqueous and non-aqueous solution (CH_3OH). In the steady state the reaction scheme may be summarised as

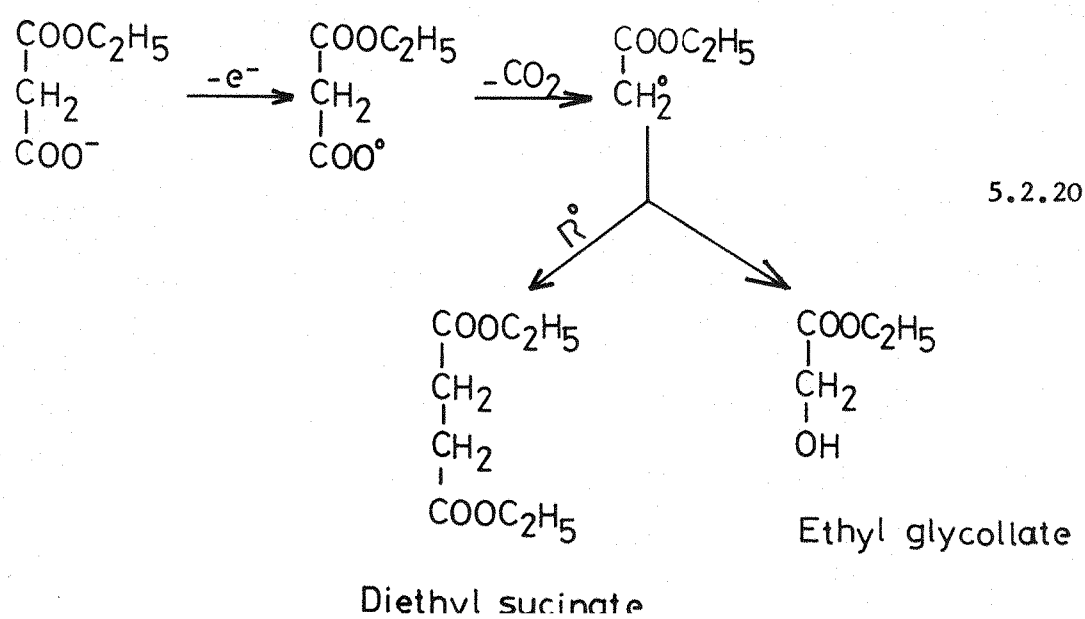

5.2.20.

However, in the non-steady state in which radicals were formed at high anodic potential followed by reduction of surface it was found that ethyl acetate was a major product. The formation of this species can be explained by reduction of the radical to a carbanion

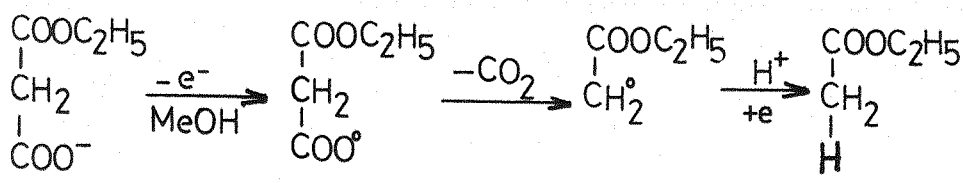

5.2.21.

before dimerization and indeed it was shown that ethyl acetate could be obtained by maintaining the electrode at a positive potential below that required to form Kolbe products in the steady state followed by reduction.

The aim of this investigation was to seek to establish conditions under which the carbanion might be coupled with other species.

III EXPERIMENTAL

A. Instrumentation

All electrochemical experiments were carried out using a chemical electronics potentiostat. A 140/2A valve potentiostat with a response time of 1μs was used for all non-steady state experiments while a transistor potentiostat TR 70V/2A was occassionally used for steady state electrolysis. A chemical electronic pulse waveform generator Type RB1 was used to generate the square wave forms for pulse electrolysis experiments. An electronic integator was used for coulometric measurements.

B. Analytical Techniques

The electrolysis solution was removed from the cell by a pipette; it was saturated with sodium chloride and shaken with the aliquot of ether three times. The ether extract was dried over anhydrous sodium sulphate and the volumetric flask was covered with aluminium foil in order to inhibit peroxide formation.

i. The main techniques of qualitative analysis was VPC-mass spectrometry, from which initial indications as to the type of product were obtained.

ii. The principal method for the quantitative analysis of the products was vapour-phase-chromatography on a PYE 104 dual column instrument using flame ionization detectors. Products were confirmed by the comparison of retention time with a known standard samples under different sets of conditions.

iii. V.P.C. - analysis.

A variety of columns was tested as to their suitability for analysis of the extremely small concentrations involved, down to 10^{-6} M. Eventually three or four columns were used for the analysis of the electrolysis solution one for high temperature, one for hydrogen bonding compounds and one for low boiling point products.

The columns and conditions used are detailed below:

COLUMNS	CONDITIONS	COMP. DETECTED
1. 20% PPG/20%diglycerol on JeJ'S "C" 100 - 120 mesh celite	flow rate 60ml/min N_2 temp. 60^oC	ethyl acetate methyl acetate methanol
2. 10% PEGA on JeJ's "C" 80 - 100 mesh celite	flow rate 60ml/min N_2 temp. 60^oC	diethyl succinate and unknown compounds
3. 20% SE-30 on JeJ's "C" 100 - 120 mesh celite	flow rate 60ml/min N_2 a) temp. 120^oC b) temp. 60^oC	a) diethyl succinate b) ethyl acetate

C. CHEMICALS

a) Triply distilled water

Water was taken from a MANESTY still.

b) Methanol

Analar methanol (99% B.D.H.) was distilled twice, dried by anhydrous magnesium sulphate and the middle fraction was collected.

c) Diethyl ether

Diethyl ether supplied by May and Baker Ltd., has a fairly high ether peroxide content in some batches. This peroxide on contact with water, easily decomposed to give acetic acid and other products. Therefore the ether used for extraction was distilled and the middle fraction taken and stored in a dark glass bottle in the fridge.

d) Monoethyl malonate, potassium salt

Monoethyl malonate, potassium salt was supplied by Fluka A.G. (99% purified) and used as supplied.

e) Ethyl bromide

Supplied by Hopkin and Williams was distilled twice and the middle fraction collected.

f) Decon 90

Initially, glassware (cells) was soaked in Decon 90 overnight, washed with distilled water and then dried in an oven at 200°C.

D. CELLS

For steady state preparative electrolysis a 25ml capacity cell was employed similar to that in fig. 1. except for the addition of a glass cooling jacket. The cell was also used for pulse electrolysis studies. The working electrode (W.E.) and secondary electrode (S.E.) were separated by a sheet of anion exchange membrane, held in place by flange and clips. The membrane Permaplex A-20 was used for all work in aqueous and methanolic solution. Sulphonated polytetrafluoroethylene membranes were also used.

E. ELECTRODES

The working electrode (W.E.) and secondary electrode (S.E.) were platinum sheet and their areas were approximately 1 sq.cm. each. The reference electrode (R.E.) was a saturated calomel dip electrode (S.C.E.) supplied by Radiometer of Copenhagen.

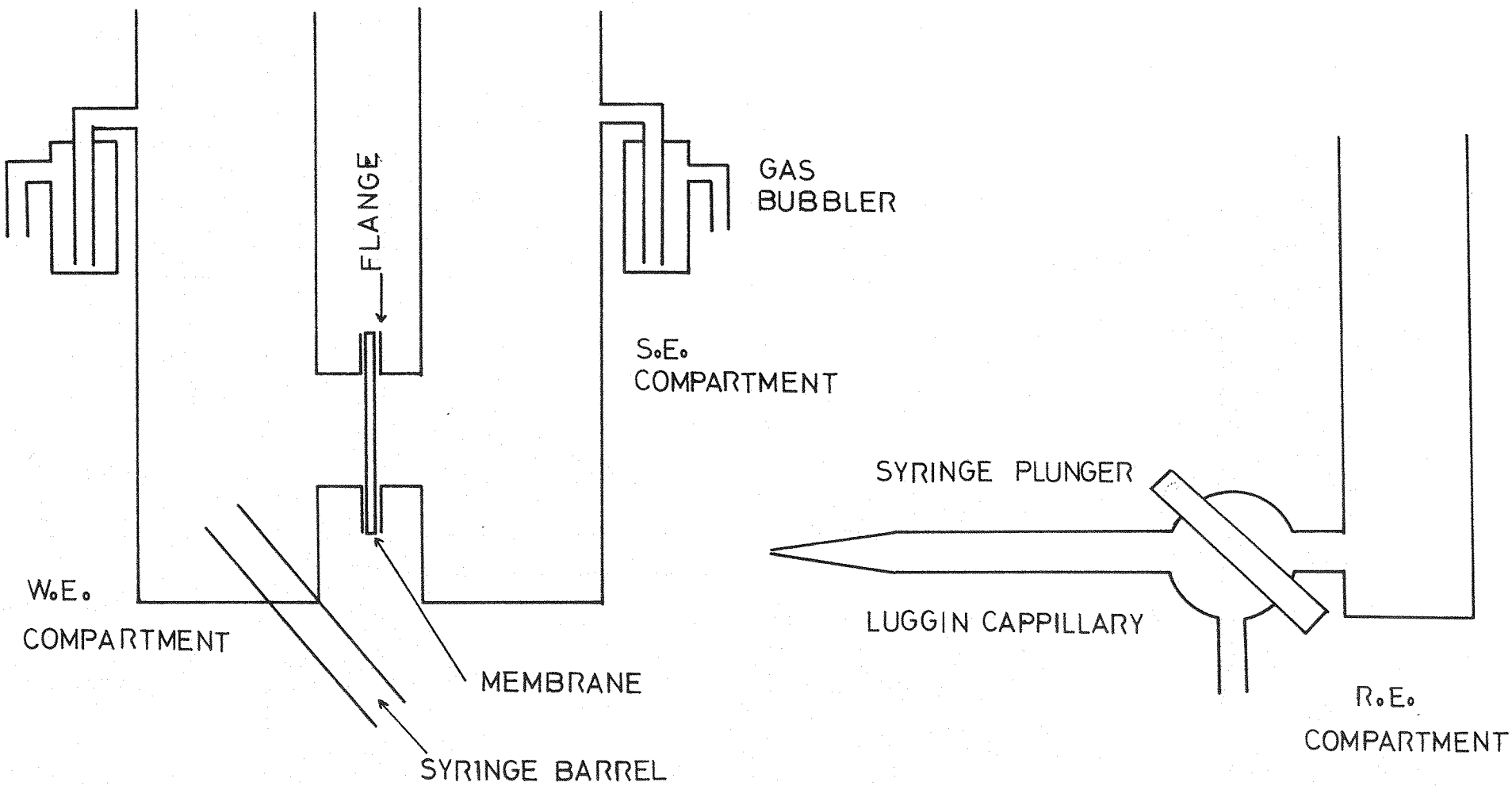

Fig.1 ELECTROLYSIS CELL

Results and Discussion

Controlled potential oxidations were carried out at four different potentials (2.8V, 3.0V, 3.2V and 3.6V) for solutions of 0.1M monoethylmalonate in water and methanol.

Figure II shows a typical plot of current versus charge passed (measured with an electronic integrator) for one of these electrolyses. As expected for an electrode process where there are no complications from slow homogeneous chemical reactions, this plot is linear. At the end of the electrolysis the solutions were analysed by V.P.C. and V.P.C/mass spectroscopy. Figure III shows a V.P.C. trace for the anolyte at the end of the electrolysis and Figure IV shows a V.P.C. trace for a standard solution of diethyl succinate; it can be seen by comparison of the retention times that the major product of the electrolysis is diethyl succinate although there are also some minor products at shorter retention times which were not identified. A V.P.C/mass spectrum of the major product had a parent peak at $\frac{M}{e} = 174$; this further confirms that this product is diethyl succinate. The yield of diethyl succinate as a function of potential is reported in table I. Brown's data[11] for the same electrolyses are also given and it can be seen that there is good agreement.

It was thought that the diethyl succinate arises by dimerisation of an adsorbed radical intermediate. If this is the case it should be possible to reduce the radical to a carbanion using a suitable pulse sequence. In an attempt to synthesis the carbanion by this route, pulse electrolyses of 2-3 hours duration were carried out using 0.1M solution of the potassium salt of monoethyl malonate and the pulse profile indicated in fig. V. This pulse profile was

It was hoped that (i) varying the potential of the reduction pulse would allow the determination of the potential of the radical/carbanion couple (ii) by shortening the length of the cathodic pulse (with the anodic pulse length being kept constant), it would be possible to reduce the radical at the surface without reducing the oxide layer. These experiments were inconclusive. Similarly attempts to trap the carbanion with ethyl bromide

$$C_2H_5O_2CCH_2^- + C_2H_5Br \text{ —— } C_2H_5O_2CCH_2C_2H_5 + Br^-$$

did not give synthetically interesting results.

It is of interest that the yields of products formed can be explained by the repeated formation layers of radicals where each radical subtends an area of 25-30 square A^o. This area is rather larger than that which would be indicated by the adsorption of a single methylene group with the ester group forming a non-adsorbed tail.

Although these experiments therefore led to the definition of the conditions under which radicals derived from monoethyl malonate could be reduced, the yields were low and it did not seem feasible to extend the synthetic applications of such systems. The project was therefore discontinued.

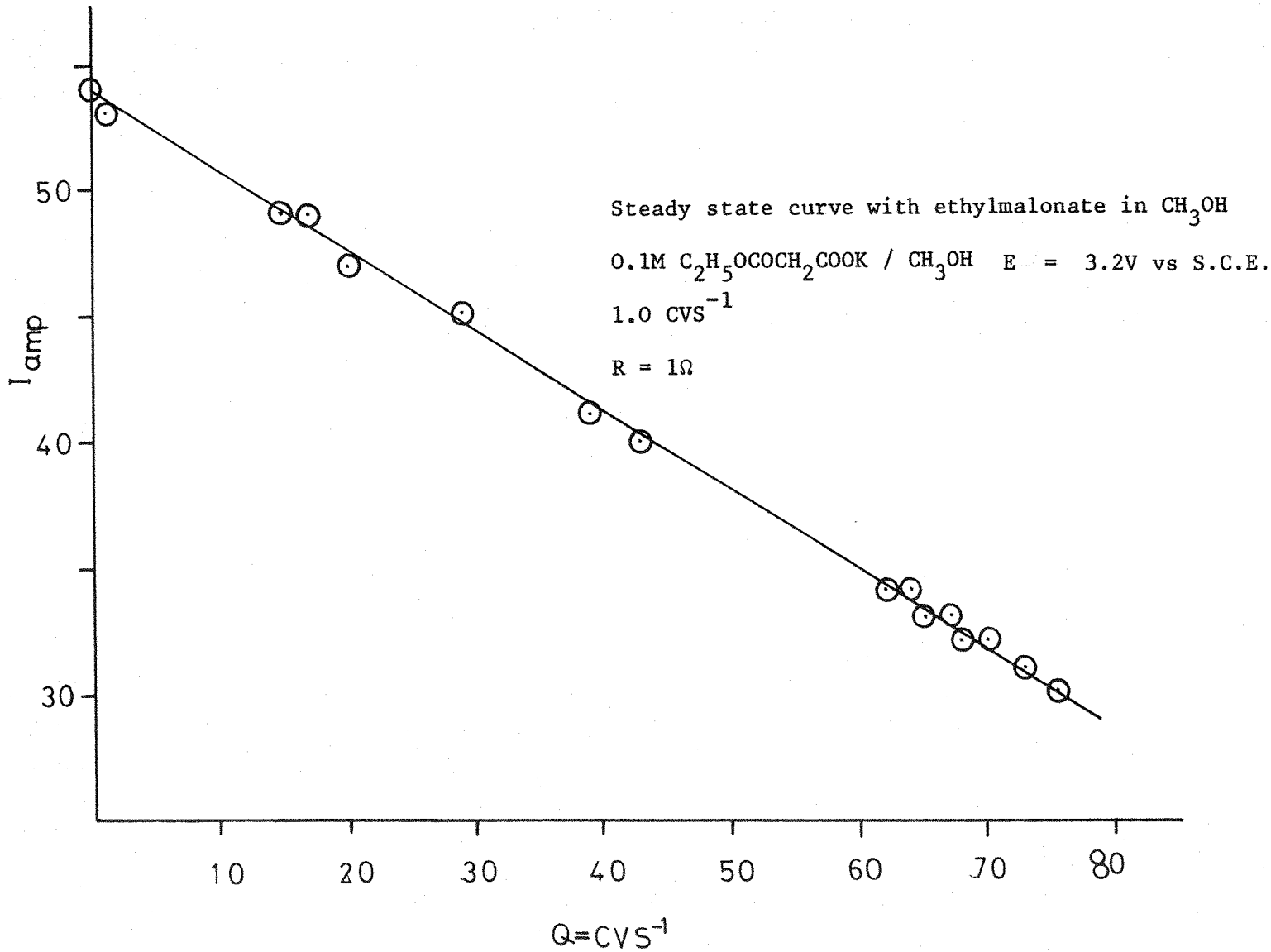
Steady state curve with ethylmalonate in CH_3OH
0.1M $C_2H_5OCOCH_2COOK$ / CH_3OH E = 3.2V vs S.C.E.
1.0 CVS^{-1}
R = 1Ω
I_{amp}
50
40
30
10
20
30
40
50
60
70
80
$Q=CVS^{-1}$

FIG. 2

Product of GLC chart of Diethyl succinate
ETHER
unknown
impurity
Diethyl succinate
0
10
20
30
40
50
60
70
80
90
100
No. 490912
PRINTED IN ENGLAND 8/78
SENSITISED COATINGS LTD. COULSDON, SURREY.

FIG. 3

Standard chart of GLC of Diethyl succinate
Ether
unknown
Diethyl succinate
impurity
0
10
20
30
40
50
60
70
80
90
100
No. 49612
PRINTED IN ENGLAND 2/78
SENSITISED COATINGS LTD. - COULSDON - SURREY.
COATINGS LTD. - COULSDON - SURREY.

FIG. 4

TABLE 1

Experiment	Potential E in V	Solvent	Conc. of CH_3OH	% yield of $(CH_2COOC_2H_5)_2$ C.J. Brown[11]	% of $(CH_2COOC_2H_5)_2$ This work
Oxidation	2.8	H_2O	0.1M	-	76.0
Oxidation	3.0	H_2O	0.1M	∿80.1	80.0
Oxidation	3.2	H_2O	0.1M	86.0	80.0
Oxidation	3.6	H_2O	0.1M	90.0	90.0
Oxidation	3.6	CH_3OH	0.1M	-	88.0

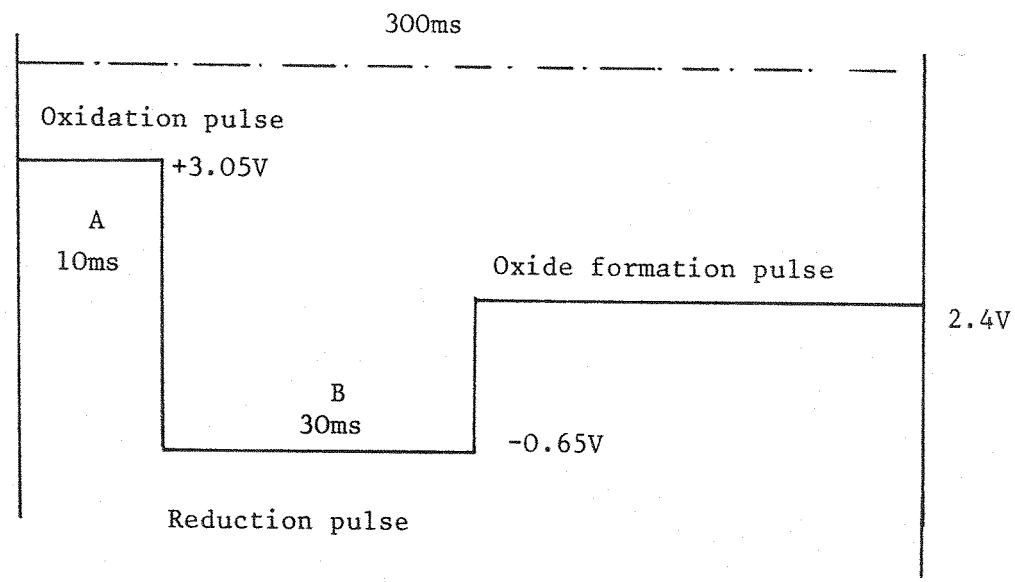

FIG. 5 Pulse profile 1:3:26

constructed in such a way as to prevent formation of radical on an oxide free platinum surface since it was feared that this might lead both to complete degradation products and to ensure that the surface conditions were identical during each pulse. It was therefore decided to use a long pulse to produce the platinum oxide followed by a short pulse into the anodic potential region where dimer formation had been shown to occur. The final part of the pulse sequence is at a potential where oxidation of the radical to carbanion is to be expected. The ratio of the various levels were chosen to be 1:3:26 while the repetition time was 300ms. The current efficiency for the dimer formation was approximately calculated from the current time transients.

At the end of these pulse electrolyses, the resulting solutions were again analysed by V.P.C. and V.P.C/mass spectroscopy. Figure VI shows V.P.C. traces for an electrolysis solution and for a standard solution of ethyl acetate, the product expected from the carbanionic intermediate

$$C_2H_5O_2CCH_2CO_2^- \xrightarrow{-e\ -CO_2} C_2H_5O_2CCH_2^{\cdot} \xrightarrow{+e} C_2H_5O_2CCH_2^- \xrightarrow[\text{solvent}]{H^+} C_2H_5O_2CCH_3$$

Comparison of retention times suggests that ethyl acetate is indeed formed and this was confirmed by mass spectroscopy, see figure VII.

The yields of ethyl acetate are reported in table II. These show that even using such a long oxide formation pulse followed by a short pulse at high anodic potential, the yield of the product from the carbanion is always very low (not more than 20%).

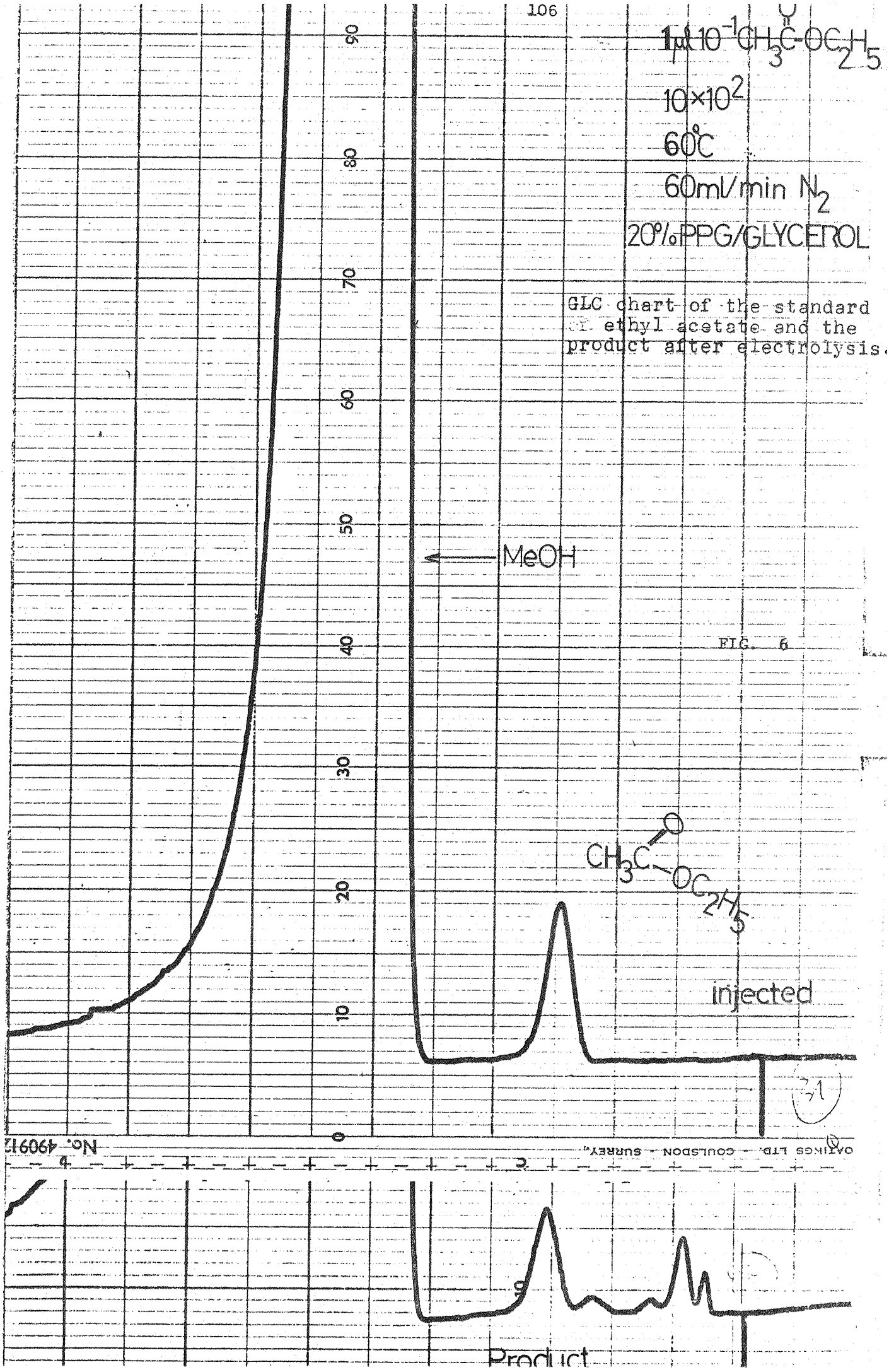

GLC chart of the standard of ethyl acetate and the product after electrolysis.

FIG. 6

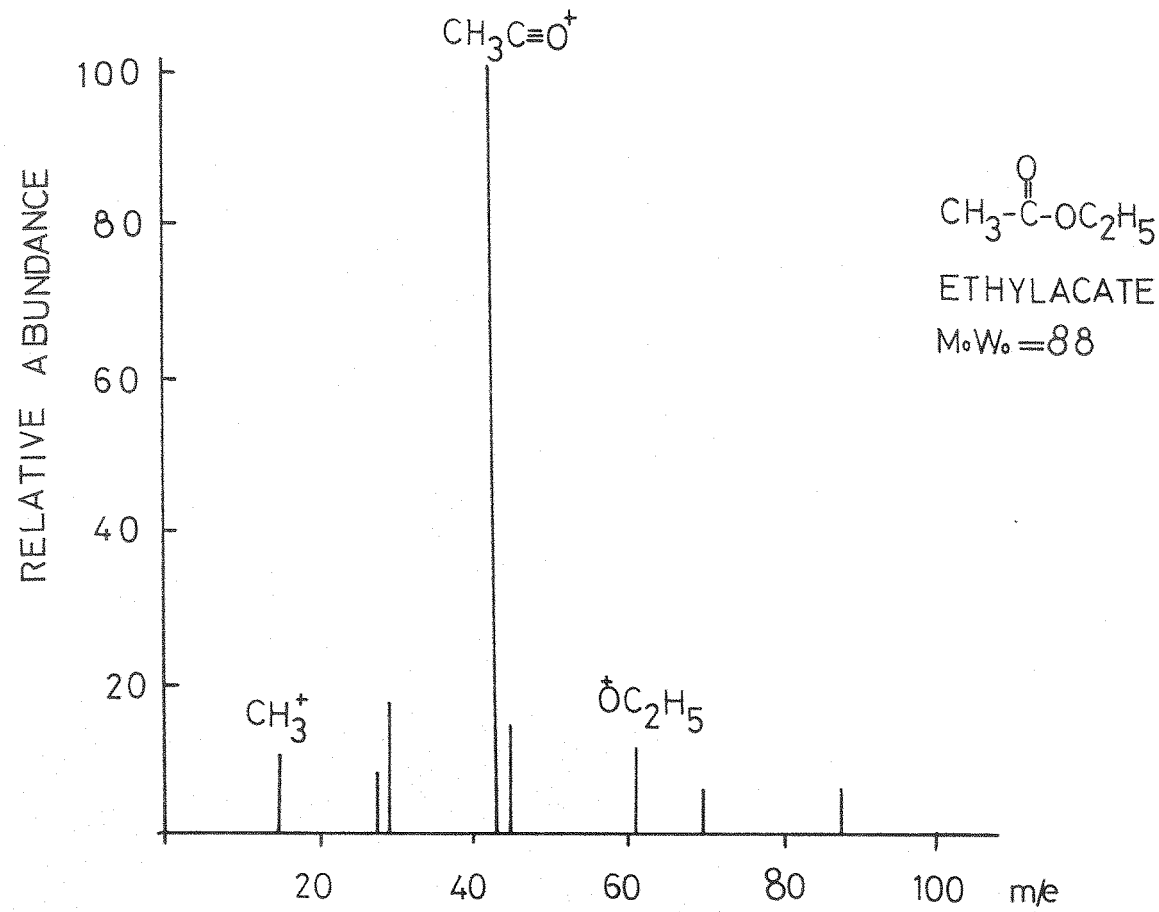

FIG. 7 The Mass Spectrum of Ethyl Acetate

TABLE 2

Materials	conc.	solvent	E	products	% yield.
$CH_3CO_2CH_2COO^-$	0.1M	CH_3OH	2.4V	methyl acetate	17.0
$C_2H_5CO_2CH_2COO^-$	0.1M	CH_3OH	2.4V	ethyl acetate	24.0
$C_2H_5CO_2CH_2COO^-$ and C_2H_5Br	0.1M	CH_3OH	2.4V	ethyl acetate	8.0

E = potential of electrolysis.

All the experiments were using the same profile as fig. 2.

REFERENCES

1. M.Faraday - Pogg.Ann. 33 438 1834
2. W.J.Koehl - J.Am.Chem.Soc., 86 4686 1964
3. V.D.Parker - Chem. Comm. 1164 1968
4. S.Sata and T.Sekini - J.Electrochem.Soc., 115 242 1968
5. Lamgmuir -
6. M.Fleischmann ε F.Goodridge - Diss.Faraday Soc., 45 254 1968
7. G.Atherton and M.Fleischmann - Trans.Faraday Soc., 63 1468 1967
8. M.Fleischmann, Lord Wyne-Jones et al - Electrochimica Acta 12 967 1969
9. M.Fleischmann and J.R.Mansfield - J.Electroanal.Chem 10 522 1965
10. H.Hofer and M.Moest - Ann. Chem., 323 285 1902
11. D.J.Brown - Thesis of Ph.D. Southampton University 1973